Methods for Characterizing Zeolite Acidity

W. E. Farneth

E.I. duPont de Nemours and Company, Central Research and Development Department, Experimental Station 356/307, Wilmington, Delaware 19898

R. J. Gorte*

Department of Chemical Engineering, University of Pennsylvania, Philadelphia, Pennsylvania 19104-6393

Received August 1, 1994 (Revised Manuscript Received November 29, 1994)

Contents

Introduction

Zeolites seem destined to become the medium of choice for a wide spectrum of selective reactions and adsorptive separations. The range of known framework compositions and pore sizes continues to rapidly expand, and with it, the range of reaction chemistries that can be carried out inside zeolite pores. On the other hand, the development of quantitative structure/activity relationships for chemistry in zeolites lags behind new materials preparations. Catalytic cracking is a case in point. Zeolites have been widely used as hydrocarbon catalysts since the early 1960s. Yet, 30 years after their introduction, while broad generalizations are clear—hydrocarbon reactions in zeolites are acid catalyzed and mediated through carbocationic intermediates—relating activity and selectivity to specific compositional and structural features of zeolites is still largely a qualitative, conjectural enterprise. The field needs ways to generate realistic potential energy surfaces for reactions in zeolites.

A real problem is the lack of an acceptable scale of solid acidity comparable to pK_a scales for aqueous solutions or proton affinities for gas-phase acid/base reactions. A primary goal of our work has been to develop structural models and experimental methods that can make direct thermodynamic links between acid/base chemistry in zeolites and the vast body of thermodynamic data on proton transfer reactions in the gas phase. In this article we will describe some of these experiments. We will try to present the work within the context of developments throughout the field of acid-catalyzed zeolite chemistry. However, the general subject of acidity of zeolites has been reviewed several times and our main goal will not be to comprehensively review it. We will instead focus on giving a thorough and cogent presentation of some of the ideas that we have found to be most helpful in understanding our work, particularly those related to quantifying acidity. We hope that the impression that the paper leaves will be of a field with exciting prospects for the future as the sophisticated use of powerful tools like solid-state NMR and microcalorimetry begin to make connections with calculational approaches to intrazeolite chemistry.

Acid/base reactions are probably the most universal class of chemical reactions. Acid/base classification systems are profitably applied in all areas of chemistry from biochemistry to heterogeneous industrial chemistry. As a result, there are a number of definitions of acid and base that have been developed through the years. Among the ones most familiar in solid acid chemistry are those due to Brønsted, Lewis, and Pearson.[1] Although there is no doubt that Lewis' and Pearson's concepts are applicable to some zeolite reactions, our focus will be on proton-transfer reactions. This leads to the first ground rule of the paper. (I) In this paper we will use the Brønsted definition of an acid: "An acid is a species with a tendency to give up a proton." [2] Brønsted acidity is

0009-2665/95/0795-0615$15.50/0

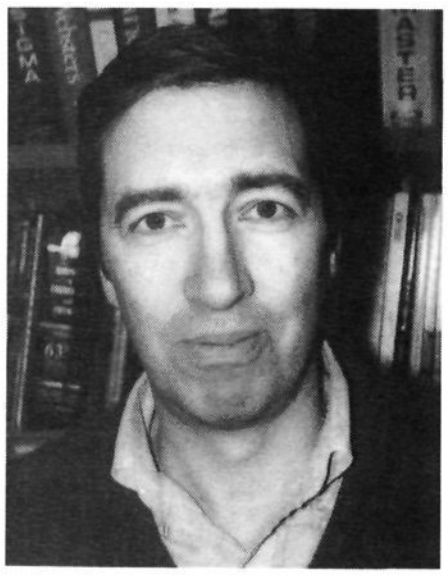

William E. Farneth is a Senior Research Associate in the Chemical Sciences Division of the Central Science and Engineering Department of the DuPont Co. He joined DuPont in 1983 after several years as an Assistant Professor of Chemistry at the University of Minnesota. He received a B.S. in Chemistry from Cornell University in 1971, a Ph.D. from Stanford University in 1975, and carried out postdoctoral research at Columbia University. He is interested in understanding how chemical reactions work, especially under heterogeneous conditions. This interest has led him to work in a variety of areas of mechanistic chemistry including: surface chemistry of solid oxides and acids, degradation reactions of polymers, semiconductor photocatalysis, laser-induced chemistry, and redox reactions of cuprate superconductors.

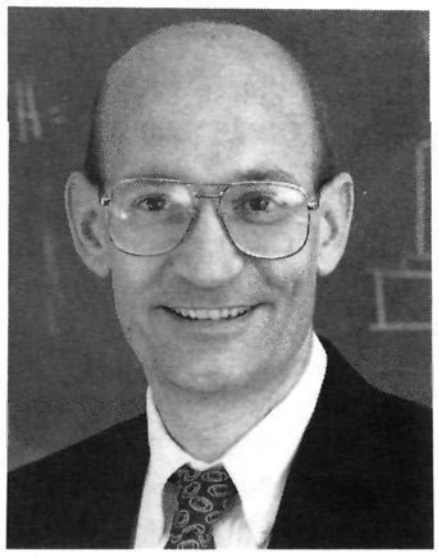

Raymond J. Gorte is a Professor and Chairman of Chemical Engineering at the University of Pennsylvania, where he has taught since 1981. He received his B.S.Ch.E. degree from the University of Wisconsin in 1976 and his Ph.D. in Chemical Engineering from the University of Minnesota in 1981. In addition to his interests in zeolite acidity, he is also studying metal-support interactions, with application toward automotive emissions control. Common themes in both areas of research are the measurement of adsorption properties of simple reactants under controlled conditions and determination of the relationships between adsorption properties and catalytic performance.

a quantifiable, thermochemical concept. Ways of quantifying Brønsted acidity have a long history in solution- and gas-phase systems. We believe that any useful quantification of solid acids must relate to this preexisting body of thermochemical data. Our preference is to correlate to gas-phase proton affinities because (1) a hypothetical proton affinity of an isolated proton acceptor site in a zeolite matrix can, in principle, be calculated by current theoretical methods, and (2) when gas-phase data are applied to solution-phase proton-transfer reactions, fundamental insights into the relative importance of the isolated chemical structures of acid and base versus their interactions with the solvent matrix have been obtained.[3] We would hope to be able to do the same thing—separate local from bulk thermodynamic influences—for proton transfer in zeolites. A number of theoretical papers have also been advancing this point of view.[4,5]

It can be difficult to separate the independent chemical and thermodynamic effects of Brønsted and Lewis sites in a solid acid system that may contain both. Most of the techniques that have proven to be useful in probing acid/base chemistry cannot easily discriminate between Lewis and Brønsted sites, so that no single characterization technique can tell you everything you need to know in order to do this unambiguously. This leads to the second ground rule. (II) We will devote most of our effort to reviewing work in which some appropriate combination of experimental techniques has been applied so that the effects of Brønsted and Lewis acidity can be differentiated. This ground rule will have the effect of emphasizing work on H-ZSM-5 and related high silica zeolites where evidence for the dominant role of Brønsted sites is most compelling. It will also have the effect of overemphasizing our own work since this is the one place where we know enough so that we can address the Lewis/Brønsted issue with some authority. It will mean unfortunately, that we do not cover work on many of the catalytically most important systems since there is evidence that catalysts optimized for activity in key hydrocarbon reactions may have both proton-donating (Brønsted) and electron-accepting (Lewis) functionalities.

The gas-phase proton affinity of a molecule M is defined as the negative of the enthalpy change for the hypothetical reaction

$$M + H^+ \rightarrow MH^+ \qquad (1)$$

in isolation from its surroundings. The corresponding free energy change is referred to as the gas-phase basicity of M. In practice, experimental determination of proton affinities involves the measurement of proton-transfer equilibria between two gas-phase bases:[6]

$$M + NH^+ \rightleftharpoons N + MH^+ \qquad (2)$$

Measured equilibrium constants for (2) directly lead to the difference in gas-phase basicity of M and N and, if the entropy change can be estimated, differences in the proton affinity. If the absolute proton affinity of M is established independently, then the measurements of $K_{(2)}$ establishes the proton affinity of N. Many measurements of this type have been made and vast compilations of the resulting proton affinities are available from a number of sources.[7]

In solution, quantitative scales of Brønsted acidity are again based on the determination of equilibrium constants for reactions like (2). In the best known acidity scale, the pK_a scale, one of the bases, say M, is water. Thus solution-phase acidities are not intrinsic properties of individual molecules, but instead measure the relative proton-donating ability of the molecule N to the reference base, water, within the medium water. By combining gas-phase proton affinities with solution-phase pK_a measurements Arnett, Taft, and others have shown how proton-transfer enthalpies or free energies can be understood as a combination of molecule specific and medium specific thermodynamic quantities.[3,8] The basic idea is illustrated in Scheme 1. Here, P represents any

Scheme 1

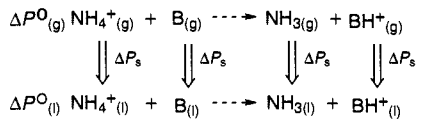

Scheme 2

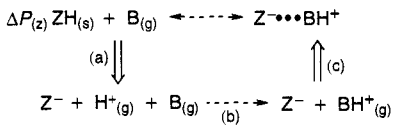

thermodynamic quantity. The horizontal changes in P, $\Delta P°(g)$ and $\Delta P°(l)$, are obtained from gas-phase and solution equilibrium measurements. The vertical changes represent solvation energies or enthalpies for each of the components of the equilibrium. By using this type of analysis, many important insights into the fundamental forces behind proton transfer have been obtained. As an example, consider HCl. The gas-phase proton affinity of Cl^- is 1393 kJ/mol, while that of H_2O is 724 kJ/mol. Therefore, the equilibrium $HCl + H_2O \leftrightarrow H_3O^+ + Cl^-$ is 669 kJ/mol endothermic in the gas phase. The pK_a of HCl is −7, representing an enthalpy change for heterolytic dissociation in water solution of roughly 42 kJ/mol exothermic. Clearly the solvation terms in the thermochemical cycle about are similar in magnitude and opposite in sign to the intrinsic terms and the details of the interactions between water and the components of the equilibrium, HCl, H^+, and Cl^-, must be understood in order to understand why HCl is a strong solution-phase acid.

One can, in principle, apply the same formalism to solid-phase proton transfer reactions. Thus a related thermodynamic cycle would be as shown in Scheme 2. Here $\Delta P_{(z)}$ represents a potentially measurable quantity, the enthalpy for proton transfer within the zeolite matrix. $\Delta P_{(z)}$ is subdivided into three components. The vertical leg (a) represents a hypothetical gas-phase affinity of a zeolite Brønsted acid site, ZH. This is not a measurable number, but it can be estimated from calculations.[9] What needs to be calculated is the heterolytic bond dissociation energy of a framework Al−O(H)−Si site. The horizontal leg (b) represents the gas-phase proton affinity of the probe molecule, B. The second vertical leg (c) represents the hypothetical enthalpy change for the process of bringing together the conjugate base of the zeolite acid site and the protonated probe molecule, from infinite separation to an equilibrium structure.

It is, of course, a difficult matter to measure an equilibrium constant like that represented by $\Delta P_{(z)}$ above. If it could be done for a variety of zeolites with the same base, one would generate a scale of solid acidities comparable to the water-based pK_a scale in that it would include both proton-transfer and solute/solvent interaction contributes for a specific reference base. What is wrong with that? Why subdivide the overall enthalpies into all of these hypothetical thermochemical quantities? It seems likely that, because of differences in the pore size and compositions in zeolites, acidity scales based on free energies of proton transfer to a specific base will vary with the choice of reference base. ZH may be a stronger base than Z'H on a scale based on ammonia, but a weaker acid on a scale based on pyridine. There is already data that suggests these types of inversions in relative acidities of different zeolites with different bases.[10] Because of these variations, scales based directly on these equilibria are unlikely to accurately predict proton-transfer thermochemistry to bases other than the reference base itself. Ultimately, a base-independent solid acidity scale, like that represented by leg (a) of Scheme 1, should lead both to more structure/activity insight and a more predictive picture of the thermochemistry of proton transfer-induced reactions in zeolites.

So how might one get there? There are many problems with trying to apply a formalism of this type to acidity in zeolites. The first is that zeolites are not molecules with a single type of acidic proton but rather collections of proton donor sites within a continuous framework. There may be a range of proton affinities for a given zeolite. Furthermore those proton affinities may change with loading. For example, the proton-donating ability of a given ZH may depend on whether nearby sites are in the BH^+/Z^- or ZH form, or interactions of BH^+ with extra-stoichiometric B molecules may alter the equilibrium constants. Much of the work that we will describe has to do with addressing these kinds of issues. Some of the experiments might be thought of as asking the following questions: Does it make sense to think of a zeolite matrix as a collection of isolated proton transfer sites? What methods can be employed to test this idea? How does the thermochemistry of proton transfer vary with coverage? How can one relate experimental measures of acidity to theoretical calculations?

The review will be presented in three sections. The first section, "Experimental Methods in Investigations of Zeolite Acidity", will be a guide to the literature on standard approaches to the quantification of Brønsted acidity in zeolites. Most of these experimental methods have been recently reviewed; therefore, we believe it is most valuable for the reader for us to first cite leading references which can be consulted for a detailed look at the technique and its history, and then add a few comments from our own experience with the application of each technique to standard materials like H-ZSM-5. In the next section, "Stoichiometric Adsorption Complexes at Acid Sites in Zeolites", we will document results from our laboratories utilizing a combination of these approaches that have led us to conclude that carefully prepared H-ZSM-5 can be profitably described as a collection of isolated, uniform (within the power of any of these techniques to discriminate), proton-donor sites. The final section, "Structure/Activity Models Starting from Stoichiometric Complexes," will discuss how that description of the nature of H-ZSM-5 as a solid acid, along with the proton affinity concept, can then be used as a starting point for potential energy descriptions of acid-catalyzed reactions in zeolites. We will show how it is especially well suited to link recent progress in NMR of reaction intermediates, with rapidly improving theoretical approaches, to intrazeolite chemistry.

Experimental Methods in Investigations of Zeolite Acidity

IR Spectroscopy

Infrared spectroscopy is the starting point for a comprehensive examination of zeolite acid sites. Both direct characterization of the H-zeolite form, especially O−H stretching frequencies, and the spectroscopic changes observed when small molecules are adsorbed give useful information. Pyridine titrations are particularly useful since the assignments of modes associated with pyridinium ions formed in Brønsted sites, and coordination complexes at Lewis sites, are well established.[11] Quantitative analysis of site densities is also possible on the basis of literature values for molar extinction coefficients in a few zeolite systems. There are several recent articles that should be consulted for details.[12,15] However, it is worth noting that some recent work leaves considerable doubt about the long-standing suggestions that O−H stretching frequencies can be directly correlated with acidities.[14-16] One can certainly identify different types of hydroxyls that appear to have different chemical activities. In the case of H-Y zeolites, for example, two hydroxyl features are observed, at 3640 and 3540 cm^{-1}. Only the higher energy feature leads to characteristic Brønsted acid chemistry with propylamines.[25] A similar situation occurs in H-mordenite.[13] In both cases, the different hydroxyl frequencies represent Al−(OH)−Si groups in channels of different dimensions. It is not clear whether the differences in reactivity result from these geometric factors or acidity differences. In steamed H-Y catalysts, the IR spectra are much more complicated, probably due to the presence of nonframework material which also contain hydroxyls, although there is again some evidence that only particular hydroxyls contribute significantly to the reactivity.[26] Thus, a more complex picture seems to be emerging in which the clear correlation is between O−H stretching frequencies and Al−(OH)−Si bond angles.[16,17] These bond angle changes may or may not represent significant proton affinity differences.

H-ZSM-5 contains at least three different types of hydroxyls. The acidic (Al−(OH)−Si) hydroxyl is observed at 3605 cm^{-1}.[18] The intensity of this band increases with Al content, and the peak disappears on exchange to obtain the ammonium form of the zeolite, NH_4-ZSM-5.[19] A second hydroxyl at 3740 cm^{-1} is observed in H-ZSM-5 and in fact on almost all silicas and is associated with isolated Si−OH at the exterior of the crystallites.[18] Most ZSM-5 samples also show a third broad feature in the IR spectrum centered at ~3500 cm^{-1}, which appears to be related to defects in the crystalline structure, possibly nested silanols which would be needed for charge compensation at a cation vacancy. The evidence that this feature is associated with crystal imperfections is 2-fold. First, ^1H-^{29}Si NMR cross polarization experiments in high-silica ZSM-5 have demonstrated the presence of significant concentrations of internal silanols.[20] Second, steaming of a high-silica ZSM-5 sharpens features in the ^{29}Si NMR spectrum significantly, allowing each of the lattice positions to be resolved.[21] This procedure also greatly reduces the intensity of the 3500 cm^{-1} IR band. It has been suggested that the 3605 cm^{-1} band is in fact a convolution of a heterogeneous mixture of Al−(OH)−Si stretching frequencies. Five bands corresponding to five different crystallographic sites have been suggested from multiple-Gaussian curve fits of spectra with adsorbed chlorobenzene.[22] However, the problem with this last approach is that hydroxylic protons can be involved in complex exchange dynamics when proton acceptors are present in the micropores, so that one cannot really be sure, without additional information, that one is examining a stable, hydrogen-bonded complex.

H/D exchange reactions on ZSM-5 reveal some of the complications that can occur in the use of IR with probe molecules to examine proton-donating sites. It is possible to exchange all three types of hydroxyls in H-ZSM-5 by exposure to D_2O vapor at 295 K.[23] Furthermore, it is possible to reexchange all three OD sites in D-ZSM-5 with the weak base, toluene, in a similar way. This D_2O, followed by toluene, exchange procedure constitutes an indirect way to determine the relative concentrations of Al−(OH)−Si (3605 cm^{-1}) and Si−(OH) (~3500 cm^1) sites when the IR observations are combined with TPD of the adsorbed toluene. In the particular case that we examined,[24] the two types of hydroxyls were present in roughly comparable amounts. We presume that type of site ratio is typical for commercial ZSM-5 materials. This ratio might have been difficult to determine directly by IR since the internal silanol band is much broader, and good extinction coefficients are hard to establish. From the toluene IR/TPD experiments, however, one should not conclude that all three types of hydroxyls are strong enough acids to have favorable equilibrium constants for proton transfer to toluene. No H/D exchange with toluene occurs on a zeolite, containing O−D silanols, which has been exposed to ammonia at a coverage of one molecule per Al. Our interpretation of this result is that H/D exchange between toluene and silanol sites (other than those associated with Al) is indirect, either occurring by exchange with protonated toluene at Al−(OH)−Si sites at high adsorbate loadings or through hydrogen diffusion on the lattice. In either case, direct proton transfer to a neutral toluene molecule from Si−OH is not possible. Issues like this, which have to do with kinetic versus thermodynamic control of the zeolite-initiated, proton transfer chemistry, arise in all of the characterization methods used to examine acidity. We will return to this question, particularly the influence of adsorbate loading and temperature, in the sections on NMR and TPD.

Alkane Cracking

The commercial utility of zeolites in the chemical process industries is largely based on their catalysis of proton transfer-initiated reactions of hydrocarbons. As a result, a vast amount literature has developed in which reactivity in hydrocarbon chemistry has been used to characterize differences, including nominal acidity differences, among zeolite materials.[27,28] Reactivity studies involving almost every type of functionalized organic molecule have also been common.[29,30] In some of these other types of reactions,

for example zeolite-catalyzed ketone condensation reactions, the link to Brønsted acidity is not so clear as in hydrocarbon cracking.[31-33] However, it is important to emphasize that, even in hydrocarbon cracking where the involvement of Brønsted acid sites is (we believe) indisputable,[34,35] proton transfer is only the initiation step of a complex matrix of competitive and consecutive reactions that ultimately lead to product. Careful reaction studies may yield information about acidity; but the terms acidity and activity are not interchangable, and careless use of these terms has made the literature in this area very confusing. Because we wish to elaborate on this point in the discussion below, we begin with a brief description of the mechanism of alkane cracking.

Mechanisms of Alkane Cracking

We will discuss cracking chemistry from the standpoint of Brønsted acid catalysis. There is significant evidence that Brønsted acid sites are primarily responsible for alkane cracking. One of the most recent and convincing demonstrations of this fact was carried out by Abbot and Guerzoni, who examined cracking rates on a mordenite catalyst which had been calcined at several temperatures in order to vary the amounts of Brønsted acid and Lewis acid sites.[35] They observed a steady decrease in the activity of the catalyst as dehydroxylation removed the Brønsted acid sites. Therefore, they concluded that the Lewis acid sites did not substantially alter the reaction rates. As we will discuss later in this section, the presence of nonframework alumina and Lewis acid sites may well affect secondary reactions, but they do not appear to be involved in the primary processes.

The basic mechanism of alkane cracking is reasonably well established, although complex. The primary process is a chainlike reaction involving carbenium ions, as shown in mechanism 1. The car-

$$R{-}CH^{+}{-}CH_2{-}R \rightarrow R'{-}CH{=}CH_2 + R^{+}$$

$$R^{+} + R'{-}CH_2{-}CH_2{-}R \rightarrow RH + R'{-}CH^{+}{-}CH_2{-}R$$

mechanism 1

benium ions can undergo C−C bond scission at the β position from the positively charged carbon, leading to an olefin product and another carbenium ion. Alternatively, hydride transfer from an alkane molecule to the carbenium ion results in a second alkane molecule and an olefin, which can then be protonated by the Brønsted-acid site to form another carbenium ion. Because hydride and alkyl shifts are facile in carbenium ions, products from these reactions are very complex.

A second reaction step, involving a nonclassical, pentacoordinated carbonium ion, appears to be important at high temperatures and low reactant pressures and may be required as an "initiation" step for producing carbenium ions when no olefins are present in the feed.[36] The nonclassical carbonium ion, formed by protonation of an alkane at the Brønsted acid site, decomposes by splitting off H_2 or an alkane to form a carbenium ion, which can then reprotonate the zeolite and desorb from the site as an olefin, or enter the chain mechanism shown above.

$$R'{-}CH_2{-}CH_2{-}R + H^{+} \rightarrow R'{-}CH_3^{+}{-}CH_2{-}R$$

$$R'{-}CH_3^{+}{-}CH_2{-}R \rightarrow H_2 + R'{-}CH^{+}{-}CH_2{-}R$$

or

$$R'{-}CH_3^{+}{-}CH_2{-}R \rightarrow R'{-}CH_3 + CH_2^{+}{-}R$$

mechanism 2

Direct evidence for the existence of this second mechanism comes from two sources. First, the reaction products, particularly H_2 and methane, formed by the reaction of small molecules like butanes and pentanes at low conversions, agrees with mechanistic expectations.[37,38] Furthermore, the formation of these products is linear with conversion at low conversions and drops off at higher conversions.[39] Second, it has been demonstrated that rapid H/D exchange of saturated hydrocarbons (3-methylpentane) in zeolites can occur under conditions in which cracking is negligible suggesting that the formation of the carbonium ion is not the rate-limiting step in cracking chemistry.[40] This in turn implies that differences in catalytic activities under cracking conditions cannot be attributed directly to differences in either rates or equilibria in the proton-transfer initiation step without the additional assumption that barrier heights for the subsequent rate-limiting bond cleavage and/or hydride-transfer steps are independent of the details of the intrazeolite environment. This seems to us to be a dubious assumption.

Variations in Activity with Zeolite Structure

Different zeolites show very different specific rates of hydrocarbon cracking, as numerous published studies have demonstrated.[41] Two extreme points of view can be taken in rationalizing results of this kind. The two opposing points of view are as follows: (1) Crystallographic Al−(OH)−Si positions in zeolite lattices, even within a single structure, come in a wide range of intrinsic acidities; these differences in proton-transfer thermodynamics control reaction rates.[42] Or (2) the intrinsic proton affinity of tetrahedral Al sites is virtually identical independent of structure or Al content;[43] activity or selectivity differences result from other unique features of reactions in micropores like geometric constraints and local concentration gradients. We believe that these two points of view cannot be reconciled on the basis of reactivity studies alone. The rates and product distributions *must* be sensitive to geometric constraints and local concentration gradients that will have major influences on the rates of the C−C bond cleavage and H-transfer steps in the mechanism above. These effects will mask any differences in proton-transfer preequilibria which may be present. In support of this assertion let us consider a specific study.

Hall et al. have contributed an especially well-controlled example of a kinetic comparison of cracking chemistry among zeolite materials. In separate papers, they examined neopentane and isobutane

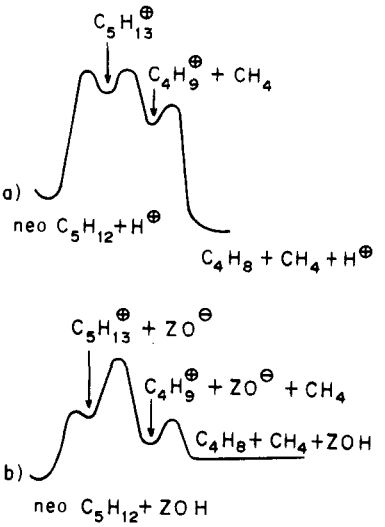

Figure 1. Potential energy diagrams for the alkane cracking reaction. The sketch in a is the proposed diagram from Hall and co-workers,[44,45] while b shows our modifications to this picture, as described in the text.

cracking.[44,45] In the neopentane work, the authors measured activation energies for CH_4 formation and the proportion isobutene in the product mixture and concluded that the activity differences among a series of catalysts could be ascribed to differences in acid strength. In the isobutane work, which appeared a little later, they demonstrated the same activity order in the same catalyst series, but were more cautious in the interpretation, preferring a noncommittal "for whatever reason" in characterizing the activity order. As a qualitative picture for how acidity differences can lead to the observed changes in cracking activity, the authors suggested an idealized potential energy diagram similar to that shown in Figure 1a. The rate-limiting step is shown to be the initial protonation step, and increasing acidity corresponds to both a drop in the overall reaction barrier, and a deepening of the potential well for the *tert*-butyl cation.

We believe that a more plausible potential energy diagram might be like that shown in Figure 1b. There are two significant changes. First, the overall reaction is endothermic. This tends to emphasize the important role that entropy must play in this chemistry even to obtain favorable overall equilibria. Second, the protonation step is shown to be reversible with a large barrier to the C–C bond-cleavage process that produces methane. The reversibility is consistent with the isotope exchange experiments referred to above. The existence of significant barriers for this type of reaction of carbon-centered cations, at least for carbenium ions, is known from mass spectroscopy.[46] In any case, if the potential surface were more like that in Figure 1b, then it is not hard to see how large differences in activity could occur for zeolites with essentially identical proton affinities. Clearly, improving our thermochemical input to these potential energy diagrams is the way to better understanding proton transfer-initiated reactions in zeolites.

Variations in Activity with Aluminum Content

Much of the early work in alkane cracking was performed on low-silica faujasites, like H-Y. One of the important conclusions reached in work on these materials was that catalytic activities increased as Al was removed from the lattice, implying that the activity per Al-substituted site increased for more dilute sites.[47] Much effort has been devoted to rationalizing this effect. Explanations include local pictures based on decreased activity for Al–(OH)–Si sites with near-neighbor Al atoms,[48] bulk models based on decreased proton-transfer rates with changes in the composite electronegativity of the framework[49] and reaction dynamics pictures based on improved intracrystalline diffusivity.[50] It is now clear, however, that the increase in specific activity with decreasing aluminum content holds only in the very low-silica content materials. For high-silica (Si/Al > 10) materials like H-ZSM-5, catalytic activities for a number of reactions, particularly cracking, increase linearly with Al content.[51] Even for faujasites, the activity per Al atom for several cracking reactions has now been shown to be constant at Si/Al > 4.5.[52] Fresh, ultrastable Y catalysts have framework Al contents in this range and equilibrium catalysts in fluid catalytic cracking reactors will have even lower amounts of framework Al due to steaming in the regeneration units. For the most industrially important high-silica catalysts, then, cracking reactivity studies imply that catalytically active sites are local structures associated with individual Al atoms in the lattice. Al atoms in lattice sites beyond the first nearest-neighbor distance apparently cannot influence the cracking activity of the Al–(OH)–Si sites or else the dependence of the specific activity of these materials should extend to lower Al contents.

The linear increase in activity with Al content does not necessarily imply that all Al–(OH)–Si sites in a given zeolite are of equivalent activity. For example, H-ZSM-5 contains 12 crystallographically inequivalent lattice positions.[53] If Al is randomly distributed among these positions, but only certain positions result in a site capable of transferring a proton to the reactant, then rates would still increase linearly with framework Al content. This has been proposed, and poisoning studies have been employed to try to demonstrate these acid strength distributions.[54] There are several variations on the poisoning technique; but, in general, reaction rates are measured on a sample which has been exposed to a strong base at a concentration less than the total Al content. The amount of base necessary to eliminate catalytic activity in some probe reaction is then correlated to the distribution of acid strengths of the Al–(OH)–Si sites in that material. Again, we believe caution is required in the interpretation of these experiments, and verification of any conclusions on acid strength distributions must be sought in other techniques. In the case of H-ZSM-5, for example, it is hard to reconcile a large distribution in site strengths inferred from ammonia poisoning of hexane cracking with the essentially constant differential heats of adsorption for ammonia that have been observed calorimetrically.[10]

Variations in Activity Resulting from Steaming

The effect of steaming on the alkane cracking activity of a zeolite is significant in both H-Y and H-ZSM-5 catalysts. Steaming, which ultimately leads to catalyst deactivation by removal of frame-

work Al, can initially increase cracking rates by a factor of 5 or more.[55,56] We mention this subject here only because it has often been associated with an increase in acidity of the zeolite. It has been suggested that nonframework Al species help stabilize the negative charge in the conjugate base of the framework Al−(OH)−Si Brønsted sites.[57] This type of stabilization effect finds precedence in solution-phase acids. Trifluoroacetic acid is a much stronger acid than acetic acid because of the inductive stabilization of the carboxylate anion by the electronegative F atoms. However, to our knowledge, it has not been proven that enhanced activity in steamed zeolites is associated with either a decreased proton affinity or a change in an equilibrium constant for proton donation to a reference base. In our own calorimetric studies of steamed faujasites, we were unable to distinguish sites in materials which showed enhanced activities from those that did not.[58] Again, enhanced "activity" could come from factors other than enhanced "acidity". A plausible alternative might involve a role for Lewis sites associated with extra framework species in hydride transfer steps that follow carbenium ion formation in the overall mechanism.[59]

Our main point in this section is that, with all of these well established effects of structure and pretreatment on activity, one should not be too hasty in ascribing them to acidity differences.

UV–Visible Spectroscopy

UV−visible spectroscopy was first used in the characterization of the strengths of solid acids by Walling.[60] Walling's method was an adaptation of the acidity function, H_0, approach developed by Hammett for determining the strengths of strong solution-phase acids. In this method, indicator bases that change color on protonation are used to probe the Brønsted acid characteristics of solid surfaces. This method has been widely applied over the last 40 years. In fact, in some early reviews of solid acids, the UV−vis based, Hammett approach is by far the most thoroughly described technique for solid acid studies.[61,62] Nevertheless, the difficulties in this approach have also been well documented, and it appears that most investigators who have examined the method in detail as a general approach to quantitative scaling of solid acids have suggested either significant experimental modifications, or have abandoned the UV−vis analysis entirely.[63-65]

While we have not used the Hammett approach in our own work and are not well versed in the experimental difficulties associated with its application, we believe that any definition of acid strength which uses solution-phase acidity data as a reference state (as the H_0 scale does) will make it much more difficult to understand structure/acidity correlations among solid acids. The problem is that solvation effects are extremely important in the overall thermochemistry of proton transfer. Thus, two reference bases with different pK_b values in aqueous solution will in general not have the same relative basicities in any other medium like the gas phase or bound to a solid surface. We have recently shown, for example, that the low-coverage differential heats of adsorption of ammonia and pyridine on H-ZSM-5 are 145 and 200 kJ/mol respectively.[10] Since it is known that both of these bases are protonated on adsorption, the binding energies reflect the enthalpies of proton transfer and the stronger base should show the higher binding energy. However, if we were to use pK_b's to predict these proton transfer binding energies, we would predict the opposite, since ammonia is by far the stronger base in aqueous media. The point is that pK_b is not an intrinsic thermodynamic property of ammonia or pyridine or methyl-substituted benzenes or nitrotoluenes or any other bases that might be used as reference proton acceptors. A more satisfactory reference state would use the gas-phase proton affinity scale as discussed in the Introduction.

UV−vis spectroscopy is also often used as a method to determine whether proton transfer has occurred during chemisorption on zeolites. Spectra characterized as polyenic carbenium ions from propene or allene have been described,[66,67] although the presence of these species had not been confirmed by other techniques.

Temperature-Programmed Desorption of Amines

Ammonia

With the possible exception of IR of adsorbed pyridine, temperature-programmed desorption (TPD) of ammonia is probably the most widely used method for characterizing acidity in zeolites. There are many variations on the method, but it typically involves saturation of the surface with ammonia under some set of adsorption conditions, followed by linear ramping of the temperature of the sample in a flowing inert gas stream. Ammonia concentration in the effluent gas may be followed by absorption/titration or mass spectroscopy. Alternatively, the experiment may be carried out in a microbalance and changes in sample mass may be followed continuously. The amount of ammonia desorbing above some characteristic temperature is taken as the acid-site concentration, and the peak desorption temperatures have been used to calculate heats of adsorption. Useful references to applications of the technique can be found in a recent review by Karge.[14]

For ZSM-5, there is no doubt that, going back to the earliest applications of ammonia TPD, it has been able to provide useful information about preparation variables, like ion-exchange conditions and deammoniation conditions necessary to optimize acid site concentrations.[68,69] Caution must be used to ensure that "physically adsorbed" species are not counted along with the ammonium ion sites. Depending on experimental conditions, like sample bed depth, carrier gas dynamics, and temperature control, desorption from nonprotonic binding sites can take place over a wide temperature range, even at temperatures approaching 600 K, where Brønsted sites are normally assumed. Deconvoluting the desorption trace to obtain Brønsted site concentrations is generally a matter of careful experimental control, but may not be possible under all conditions.

On the other hand, the determination of heats of desorption from ammonia TPD plots is not straightforward, and in spite of the large number of papers that purport to be able to extract acid strength distributions from desorption traces, the accumulated

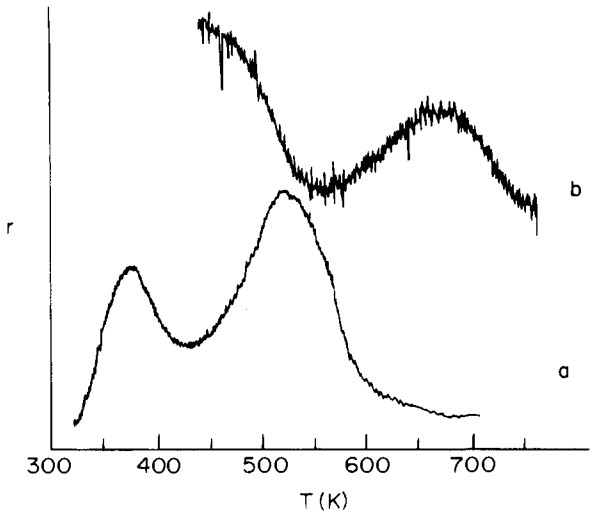

Figure 2. Temperature-programmed desorption curves for ammonia from an H-ZSM-5 sample obtained from the standard catalyst committee. Both experiments were performed in a microbalance. In a, the measurement was carried out on a 20-mg sample in vacuum with a heating rate of 20 K/min. The curve in b used a N_2 carrier and a 44-mg sample, with a heating rate of 5 K/min. (Courtesy of Mr. Erik Thiele.)

data shows little consistency. A complete description of desorption from a zeolite in a bed requires the simultaneous analysis of desorption, readsorption, and diffusion, all in the presence of a carrier gas.[70] The process is *not* greatly simplified by ramping the temperature to a fixed value and carrying out the desorption isothermally since the equations which must be solved simultaneously remain the same.

To demonstrate how important experimental parameters are in influencing TPD results, we have measured the desorption of ammonia from an H-ZSM-5 in two experimental configurations, one using a vacuum system and one using a carrier gas. The sample was obtained from the Standard Catalyst Committee and is basically a commercial ZSM-5, with a Si/Al ratio of ~32, which was calcined and ion exchanged to the hydrogen form. The results, along with the pertinent experimental conditions, are given in Figure 2. Since both measurements were performed in a microbalance, it is known that only the peak centered at ~520 K in Figure 2a and at ~670 K in Figure 2b are due to Al sites. If one were to use the common practice of assuming a first-order desorption rate with an Arrhenius temperature dependence and normal preexponential (10^{13}/s) to calculate desorption activation energies, one would get 140 kJ/mol for a and 180 kJ/mol for b, a difference of 40 kJ/mol. This analysis is obviously not an acceptable way to interpret these data, and we believe that any analysis which makes the assumption that intrinsic desorption rates can be determined from TPD on microporous materials will be in error.

When concentration gradients are not a problem, one can assume local equilibrium between the gas phase and the zeolite. The validity of this assumption was demonstrated by Dumesic and co-workers.[71] By measuring a series of TPD curves with different carrier-gas flow rates, they observed a shift in the peak temperature which could be used to calculate the average heat of desorption of ammonia from H-ZSM-5. The value they obtained was in good agreement with numbers obtained from microcalorimetry (145 kJ/mol). On the other hand, similar agreement between TPD-derived heats of adsorption and ammonia calorimetry on H-ZSM-5 has also been reported by Karge.[14] In the latter case the two methods agreed that the adsorption enthalpy was 90−110 kJ/mol. We prefer 145 kJ/mol on the basis of both our own calorimetry and on the more realistic assumptions used by Dumesic in the TPD analysis. This is, unfortunately, one of many examples of how difficult it can be to extract reliable quantitative data from this literature.

Other Amines

Our group has advocated the use of TPD of reactive amines rather than ammonia for the characterization of solid acids. Starting with H-ZSM-5, we demonstrated that well-defined, stoichiometric adsorption complexes, corresponding to a coverage of one/Al, could be obtained for a whole series of amines, including methylamine, ethylamine, *n*-propylamine, isopropylamine, and *tert*-butylamine.[72] With the exception of methylamine, the adsorption complexes could be easily identified by their reaction to olefins and ammonia in a specific temperature region in TPD which only depends on the alkyl group.[73] For example, isopropylamine at a coverage of one/Al reacts to propene and ammonia between 575 and 650 K, and this temperature range is the same for desorption in vacuum or into a carrier gas.[74] Amine molecules adsorbed in excess of one/Al desorb unreacted at lower temperatures; and the reaction temperature does not appear to depend on the composition of the lattice, based on the observation that the decomposition temperature for isopropylamine is identical on H-[Ga]ZSM-5 and H-[Fe]ZSM-5.[75,76] It appears that reaction occurs so long as the sites are able to retain the alkylammonium ion up to its characteristic decomposition temperature without desorption by reverse proton transfer.

The chief advantage of the use of alkylamines as a probe for heterogeneous acid-site densities is that the temperature-programmed decomposition reaction occurs only at Brønsted sites, not Lewis sites. On γ-Al_2O_3, for example, there is very little reaction of isopropylamine in TPD.[77] This fact helps to avoid spurious results sometimes observed with ammonia adsorption. For example, Juskelis et al. demonstrated that ammonia desorbed at a higher temperature, and with a similar specific coverage, on CaO than on typical zeolite catalysts, while no reaction of isopropylamine was observed in desorption from CaO.[74] The sites responsible for reaction of isopropylamine in TPD also appear to be responsible for hydrocarbon cracking on steamed H-Y catalysts[58,78] and amorphous silica−aluminas[77] since, in both cases, specific rates increased linearly with site densities. In another study employing amines of different sizes, it was demonstrated that TPD measurements could be used to determine the concentration of Brønsted acid sites in each of the components of a fluid-catalytic-cracking catalyst containing H-ZSM-5, H-Y, and amorphous silica−alumina.[79]

Microcalorimetry

The uses of adsorption calorimetry in heterogeneous catalysts have recently been comprehensively

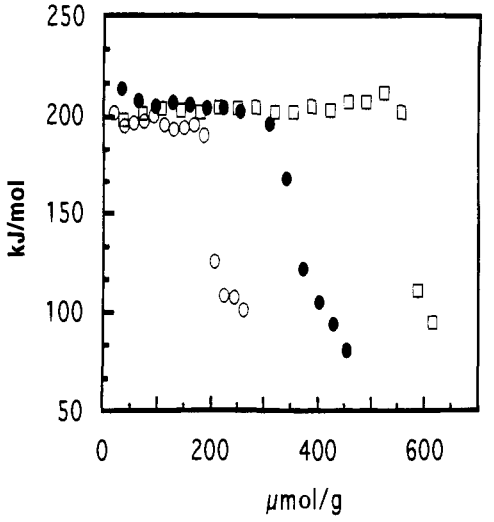

Figure 3. Heats of adsorption as a function of coverage for pyridine on three different H-ZSM-5 samples having Brønsted acid site densities of 180, 360, and 600 μmol/g, respectively. (Reprinted from ref 10. Copyright 1994 Elsevier.)

reviewed by Cardona-Martinez and Dumesic.[80] Specific applications of calorimetry to the characterization of zeolite acid sites are described both in this article and in more specialized reviews.[14,81] Adsorption calorimetry is a direct way to measure heats of adsorption of reference bases at zeolite acid sites. The usual method involves dosing of aliquots of reference base onto the solid held at a given temperature. The resulting heat pulse is collected and integrated. Dosing continues until saturation coverages are reached. The calorimetric data are usually displayed as a plot of enthalpy of adsorption versus coverage, like that shown in Figure 3. If the adsorption occurs with proton transfer, then the calorimetrically determined enthalpy of adsorption should be equivalent to ΔP_z of Scheme 2. This is clearly a key quantity in applying a thermodynamic model to the Brønsted acid characteristics of zeolites, and progress in understanding acidity in solids cannot be made without good adsorption calorimetry data of this kind.

There are, however, several inherent limitations to the technique that require that it be used in combination with other characterization methods. The first is that the nature of the binding sites cannot be known through calorimetry alone. Adsorption may occur at Brønsted sites, Lewis sites, or as a result of any combination of surface/vapor attractive forces. The second is that, even when it can be demonstrated that binding results from proton-transfer-induced adsorption at Brønsted sites on the surface of the solid, the heat of adsorption is not a measure of the proton affinity of the site. It is, in fact, a convolution of the proton affinity of the acid site on the solid, the proton affinity of the reference base, and the heat of interaction of the resulting ion pair, as represented in the thermochemical cycle of Scheme 2. Although it is common to talk about using calorimetry to measure distributions of acid site strengths, the differential heats are a more complicated thermochemical quantity that, in the general case, will have contributions specific to the structure of the base, the local geometry of the binding site, and the coverage of the surface. Third, a temperature must be chosen that allows sufficient mobility so that all available binding sites are sampled within the time scale of the experiment. Otherwise, the differential heats represent some type of kinetically averaged distribution rather than a binding strength distribution that can be interpreted by equilibrium thermodynamics. On the other hand, at temperatures that are too high, chemical reactions can occur, and the measured heats then become a complex mixture of enthalpies of adsorption and reaction.

It is probably fair to say that the optimum ways to use this technique to impact acidity studies are still evolving. It has often been used to infer site binding strength distributions in complicated materials, like partially dealuminated faujasites.[82] It has found clear uses in characterizing differences among binding sites on solid acids that have been prepared or pretreated in different ways.[83] However the accumulated quantitative data for $\Delta H_{binding}$ in specific acid/base systems are often not very consistent. For example, values ranging from 100 to 200 kJ/mol have been reported for the initial heat of adsorption of ammonia at 450−500 K in H-ZSM-5.[80] In some cases the reported differential heats of ammonia adsorption increase or decrease significantly with coverage.[67] In other cases they are constant up to the aluminum content of the zeolite.[10] There are similar uncertainties for pyridine in H-ZSM-5 where 140, 160, and 200 kJ/mol initial heats have all been claimed in recent literature.[10,84,85] It can be difficult to choose among these values since it is clear that the differential heat versus coverage curves are sensitive to synthetic and pretreatment conditions as well as variables specific to the calorimetric measurement itself, like gas temperature and sample bed depth. As more laboratories become involved in these measurements and comparisons of nominally identical systems become more routine, a consensus on the differential heat vs coverage data for some of these key systems should emerge.

Data which we have recently published for pyridine on three different H-ZSM-5 preparations are shown in Figure 3.[10] The samples included two that were synthesized in our laboratory at Penn using a templating agent and one that was prepared elsewhere without a template. All were pretreated equivalently. Brønsted acid site densities measured by TPD of isopropylamine are reported in the figure caption and agree well with the Al contents of the various materials. On each sample, the differential heat of adsorption is 200 ± 5 kJ/mol up to a coverage equal to the Brønsted acid site density, after which the heats fall dramatically. Similar results were obtained for ammonia for which the differential heats were 145 kJ/mol up to a coverage of one per acid site. These results are what one would expect for a Langmuir adsorption model at a single set of equivalent sites.

Solid-State NMR Spectroscopy

Solid-state NMR has already been applied to a variety of structure and dynamics problems in zeolite chemistry.[86] NMR is an extremely powerful tool for local structure characterization and new ways to use NMR in heterogeneous acid systems continue to appear.[87,88] We will restrict our attention to two specific subsets of this area, the use of proton NMR

to characterize Brønsted sites and the use of ^{13}C NMR to characterize adsorbates at Brønsted sites.

Pfiefer et al.[89] have published a recent review that covers the use of proton NMR for determining the number, strength, and accessibility of acidic protons in zeolites. The point of view taken in ref 89 is identical to what we have outlined in the introduction, and gas-phase proton affinity data are used to interpret the proton chemical shifts. A plot of chemical shifts of various OH-containing molecular species gas-phase acidities is shown to give a reasonable linear correlation. It appears that the data given in this paper would suggest an average proton affinity for H-ZSM-5 of about 1360 kJ/mol, although the conclusion is not stated explicitly in the article. This group has also argued that the chemical shifts of bridging hydroxyls in zeolites increase with Si/Al ratio up to a value of about 10. Higher Si/Al ratios produce no additional shift, implying that acid sites in all zeolites with Si/Al ratios greater than 10 have comparable proton affinities within the resolution of the measurement.[90] Other interesting applications of H or D NMR to the problem of Brøsted acid strengths in zeolites include the work of Root et al.[91] and Fraissard et al.[92]

Another rapidly expanding application of NMR in solid acid chemistry is its use in following the structures and transformations of adsorbed species. A primary goal in this area has been the structural characterization of adsorbed intermediates that may be involved in acid-catalyzed reactions, for example methanol conversion.[93-95] In all studies of this kind, careful control of temperature and especially coverage is important to interpret the spectroscopy unambiguously. (For example, one observes rather dramatic differences for acetone adsorption in H-ZSM-5 for different research groups, apparently due to the methods used for adsorption.[96,97]) We have found that samples prepared at or below a coverage of one adsorbate/Brønsted site yield detailed information about the fundamental features of acid/base interactions at the Brønsted sites. ^{13}C spectra of acetone, bound at a stoichiometry of one/Brønsted site, appear to be particularly useful in differentiating Brønsted acid binding sites among different zeolites. The zero-order band in the magic-angle-spinning spectra of acetone complexes for a variety of acidic zeolites gave narrow bands (line width at half max, <2 ppm) with distinguishable isotropic chemical shifts. As shown in Table 1, these ranged from 10.1 ppm in SAPO-5 to 18.7 ppm in H-ZSM-22.[98] Since all of these materials have relatively dilute Brønsted sites, these differences must result from local structural differences of the hydrogen-bound complexes. Other factors besides chemical shifts may prove to be even more important for understanding differences among materials. Since acetone has been shown to be localized at the acid sites in all of the materials investigated in Table 1 at room temperature and coverages below one/site, the static line width is a measure of the molecular motion at the site. Not surprisingly, the line widths in the acetone spectra are a strong function of the size of the cavity surrounding the acid sites. Data are shown in Table 1. The molecules are essentially rigid and the line width is large in H-ZSM-22 which has one-dimensional 10-ring channels. At the other extreme, the supercages in H-Y allow significant motion of adsorbed molecules, giving the narrowest line of all the zeolites examined. This information about site constraints clearly complements an approach to acid-catalyzed reactions that separates the site proton affinities from the adsorbate/zeolite framework interaction energies.

Table 1. Trace[a] of the Chemical Shift Tensor of the C-2 Carbon of Chemisorbed Acetone at 125 K Relative to the Neat Solid (taken from ref 98)

sample	chemical shift[b] at 125 K (ppm)	peak width for static spectrum at 295 K (ppm)	channel size (Å)
H-ZSM-22	18.7	230	5.4
H-ZSM-5A	16.9	200	5.6
H-ZSM-5B	16.8	200	5.6
H-[Ga]ZSM-5	16.1	200	5.6
H-ZSM-12	16.7	103	6.2
H-mordenite	15.1	103	7.8
SAPO-5	10.1	84	7.3
BeAPO-5	16.7		7.3
MgAPO-5	17.7	88	7.3
H-Y	12.9	44	13.4

[a] The trace, in general, corresponds very closely to the isotropic chemical shift. [b] Uncertainty is ±0.4 ppm.

Stoichiometric Adsorption Complexes and Acid Sites in Zeolites

In this section and the following one, we will describe mainly our own work on characterization of zeolite acidity. Most of the work has been performed on carefully prepared and activated, unsteamed H-ZSM-5 because of the relative simplicity of this material. We will discuss methods to prepare and to characterize the structure and energetics of complexes of H-ZSM-5 with adsorbate molecules at stoichiometries less than or equal to one adsorbate molecule/framework Al. Stoichiometric complexes with one adsorbate per Al can be prepared because the binding energies for a variety of adsorbates at or below one/Al is significantly larger than the binding energies at higher loadings. The extra stability derives from interactions with the Brønsted acidic protons. Therefore, the analysis of the structure and energetics of these complexes is in effect an analysis of the driving forces for proton transfer in the zeolite pores.

We first saw evidence that stoichiometric adsorption complexes could be readily formed by carrying out simultaneous temperature-programmed desorption (TPD) and thermogravimetric analysis (TGA) experiments in vacuum.[99,100] These experiments combine a microbalance and a mass spectrometer inside a vacuum chamber. The microbalance is used to follow changes in the mass of the solid during adsorption/desorption cycles, while the mass spectrometer is used to follow partial pressure profiles of gases evolving from the material during the temperature ramp. In a typical experiment, the sample was placed into the hydrogen form by ammonium ion exchange, followed by heating in situ, and exposed to adsorbate vapor at room temperature until a saturation coverage was obtained. The chamber was then evacuated to background pressures of 10^{-6} Torr or less. The residual adsorbate coverage

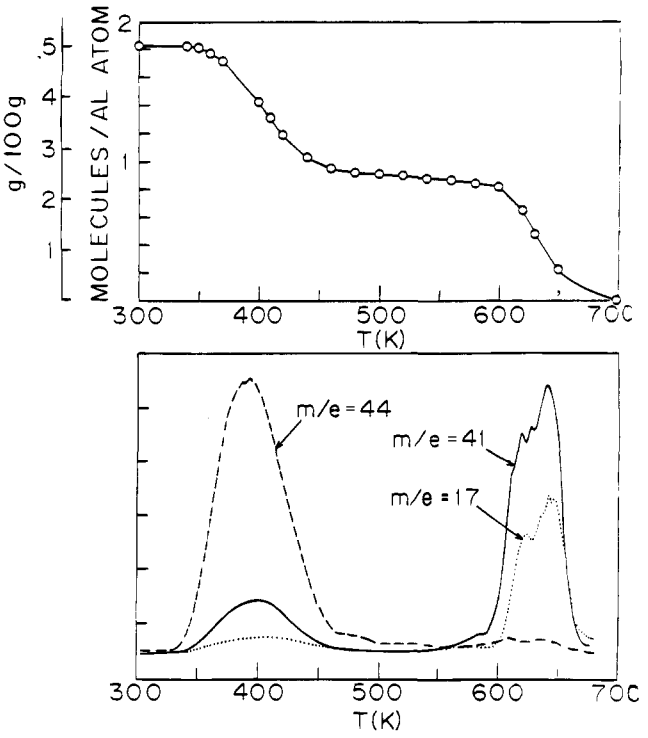

Figure 4. TPD-TGA curves for isopropylamine from H-ZSM-5. The peaks in the TPD curves indicate the formation of isopropylamine (*m/e* = 44, 41, and 17), ammonia (*m/e* = 17), and propene (*m/e* = 41). (Reprinted from ref 99. Copyright 1988 Academic.)

after evacuation depended on the particular sample and evacuation conditions. Sometimes it was essentially one adsorbate molecule/Al; sometimes it was in excess of this stoichiometry. However, in almost every case, if adsorbate molecules in excess of one per/Al remained on the zeolite at the start of the temperature ramp, they desorbed intact at lower temperatures, leaving a generally well-resolved high-temperature feature with a stoichiometry corresponding to the number of Al atoms in the lattice. The observation of clearly defined desorption features with a stoichiometry of one adsorbate per Al was made for a variety of differently functionalized adsorbates including alcohols, amines, thiols, and ketones.[72,100-102]

For many adsorbates, the molecules associated with Al undergo a unimolecular, acid-catalyzed reaction upon desorption. Typical of these is isopropylamine for which in the TPD/TGA curves are shown in Figure 4. In this case saturation and evacuation at room temperature leave behind a coverage significantly greater than one molecule/Al. However, those molecules in excess of one/Al desorb unreacted (*m/e* = 45) below 450 K. The 1:1 complex reacts between 575 and 650 K, desorbing as propene (*m/e* = 41) and ammonia (*m/e* = 17), in a reaction analogous to the well-known, solution-phase Hoffman elimination.

Infrared measurements also show that the adsorption complexes are localized at the Brønsted acid sites. The IR spectrum of clean H-ZSM-5 exhibits two sharp hydroxyl features at 3605 and 3740 cm^{-1}.[18] As stated earlier, the peak at 3740 cm^{-1} is present on all silicas and has been assigned to external silanol groups which terminate the crystallites. The peak at 3605 cm^{-1} is present only in the hydrogen form of the zeolite and its intensity is correlated with framework Al content. Upon adsorption of one molecule of isopropylamine per Al, the 3605 cm^{-1} peak completely disappears while the 3740 cm^{-1} peak is unaffected.[72] Adsorption of pyridine at coverages corresponding to the 1:1 stoichiometry shows only pyridinium ions.[72]

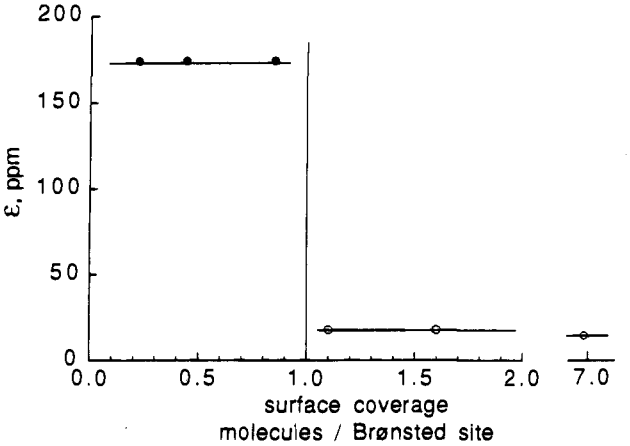

Figure 5. Line width at half maximum for the static spectrum of acetone (2-^{13}C-2-propanone) in H-ZSM-5 as a function of coverage at room temperature. (Reprinted from ref 102. Copyright 1993 American Chemical Society.)

NMR experiments illustrate the clear distinction between the structure and dynamics of adsorbates at stoichiometries less than one/Al and in excess of the 1:1 ratio. For C-2, ^{13}C-labeled 2-propanone at room temperature and coverages below one/acid site, the ^{13}C NMR spectrum exhibits a chemical shift anisotropy which is close to that of solid acetone, implying that the bound molecule is rigid on the NMR time scale.[102] At coverages even slightly above one/site, the entire line shape collapses into a narrow line, indicating that rapid exchange occurs between the physisorbed acetone and the rigid acetone on the time scale of the NMR measurements. This is shown in Figure 5, which is a plot of the peakwidth of the static spectrum as a function of coverage and demonstrates that the transition to mobility is very sharp. For coverages above one/acid site, one also observes the onset of bimolecular reactions to mesityl oxide.[97] In addition to showing that a 1:1 adsorption complex exists between acetone and the acid sites, Figure 5 also indicates that the molecules associated with the complex are localized at those acid sites at coverages below one/site, an important observation which can be used in the characterization of the acid sites, as we have already alluded to and will discuss in more detail in a later section.[33,98]

Adsorption calorimetry, like that shown in Figure 3, gives information about the enthalpic driving force for the formation of these proton-bound complexes. The differential heats of pyridine adsorption are essentially constant at 200 kJ/mol up to a coverage of one molecule/acid site and much lower at higher coverages. In this case, the difference between binding energies below a 1:1 stoichiometry and above 1:1 stoichiometry is on the order of 100 kJ/mol. Similar observations have been made with ammonia and a variety of other alkyl amines.[10,103] These experiments demonstrate the significant enthalpy advantage of binding at the Brønsted sites in ZSM-5 and the effective equivalence of these binding sites, at least at 480 K. We cannot say why other similar

calorimetry experiments on H-ZSM-5 have shown either very high initial heats, or broad distributions that do not clearly drop at the stoichiometric proton concentration.[80] We suspect that there are both measurement errors and intrinsic differences in sample microstructures (*vide infra*).

We like to think of the 1:1 adsorption complexes as being homogeneous. They can be characterized by a heat of adsorption, a local site structure, and a chemical reactivity profile. We recognize that these may be averaged quantities since Al atoms may occupy more than one type of crystallographic site in ZSM-5. However, the level of heterogeneity is not well established given the difficulties in trying to determine distributions of ZO-H acid strengths from spectroscopic or TPD peak widths or from coverage dependent differential calorimetry, as we have discussed in previous sections. Furthermore, for practical catalytic purposes, activity in unmodified H-ZSM-5 seems not to be associated with some subset of the acid sites, but rather scales with total Al content.[51] Therefore, we believe that comparing the thermochemistry, structure, and reaction properties of these 1:1 complexes across zeolite and adsorbate structures is the best way to make progress toward understanding what controls acid-catalyzed reactivity inside zeolite pores. The remainder of the review will focus on the chemical and spectroscopic characteristics of these complexes.

Structure/Activity Models Starting from Stoichiometric Complexes

Thermochemistry of Amine/H-ZSM-5 Complexes

Thermochemical data from gas-phase measurements have greatly increased our understanding of acidity and solvent effects in Brønsted acid solutions, as discussed in the Introduction. Equilibrium constants and heats of reaction for the interaction of a gas-phase base with a proton

$$H^+ + B_{(g)} = HB_{(g)}^+$$

can be determined using modified mass spectrometric methods and applied to solutions using Scheme 1. Discrepancies between gas-phase and condensed-phase proton-transfer thermodynamics can therefore by unequivocally assigned to solvent effects in the solution.[104] For example, the higher basicity of ammonia relative to trimethylamine in aqueous-phase acids is understood to be due to the more favorable solvation of the ammonium ions resulting from the formation of multiple hydrogen bonds. Trimethylamine is intrinsically (that is, in the gas phase) a much stronger base.

We believe that a similar methodology is useful for examining acidity in zeolites. To compare acidity in zeolites to gas-phase and solution-phase acidity scales, we examined the differential heats of adsorption for a series of amines in H-ZSM-5.[103] For each of the amines examined, which are listed in Table 2, the differential heats vs coverage curves look essentially the same as Figure 3. The differential heats of adsorption are essentially constant up to a coverage of one/Al, after which the heats fall dramatically. In the plateau region, therefore, the binding enthalpies, ΔH_{bind}, must be associated with the interactions of each base with the Brønsted acid sites. These values are listed in Table 2, along with the gas-phase proton affinities and the heats of protonation in aqueous-phase acids.

Table 2. A Comparison of Adsorption Enthalpies in H-ZSM-5 to Gas-Phase and Solution-Phase Basicities (taken from ref 103)

	ΔH_{bind} (kJ/mol)	PA (kJ/mol)	$\Delta H_{prot,\ S^\circ}$ (kJ/mol)
ammonia	145	858.3	52.3
methylamine	185	896.4	55.1
ethylamine	195	909.0	57.4
isopropylamine	205	918.6	58.5
n-butylamine	220	916.9	58.5
dimethylamine	205	923.2	50.4
trimethylamine	205	939.1	36.9

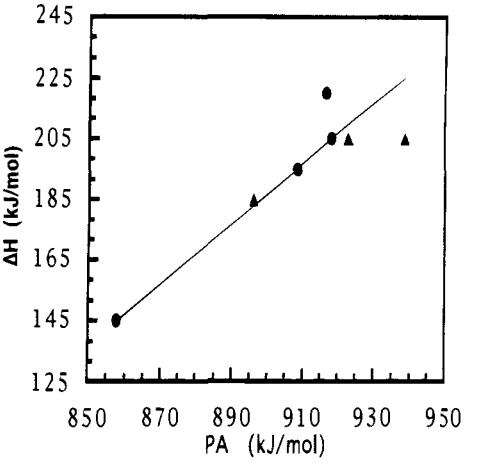

Figure 6. The average differential heats of adsorption for amines in H-ZSM-5 plotted as a function of their gas-phase, proton affinities. The line in the figure has a slope of one and intersects the point for ammonia. (Reprinted from ref 103. Copyright 1993 American Chemical Society.)

A comparison between the average differential heats of adsorption and the gas-phase proton affinities is shown in Figure 6. The correlation is excellent.[105] The line in the figure was drawn with a slope of one, and five of six molecules fall within 5 kJ/mol of that line. In contrast, there is no correlation between the heats measured in zeolites and heats of protonation in aqueous solutions. This is shown by the plot in Figure 7. In water, the total protonation enthalpies of the amines are dominated by solvation effects, and the relative basicities are controlled by specific solvation differences between the substituted amines, their corresponding alkylammonium ions, and water.[3] Even in low dielectric constant, nonhydrogen-bonding solvents, the relative amine basicities do not follow the intrinsic gas-phase order, and specific solvation and ion-pairing effects can lead to complex basicity orders that differ from the intrinsic order.[104]

It is useful to discuss the correlation in Figure 6 in terms of the thermochemical cycle in Scheme 2. Figure 6 is, in fact, a plot of $\Delta H_{binding}$ vs PA_B from Scheme 2. The linear correlation requires that the sum of the vertical legs of the cycle (i.e. the proton affinity of the zeolite, PA_{ZO^-} (a), and the intrazeolite ion pairing energy, $\Delta H_{interaction}$ (c)) be a constant for this set of bases. The sum of these two thermochemical quantities is about 713 kJ/mol. (For ex-

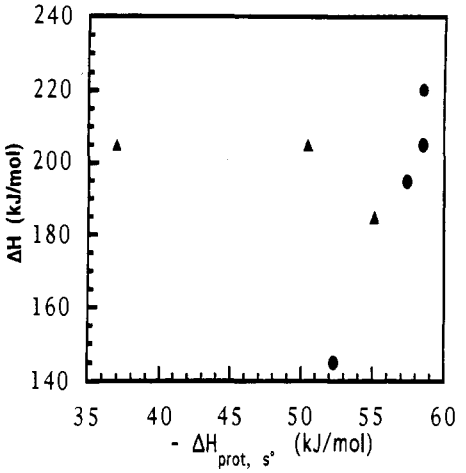

Figure 7. The average differential heats of adsorption for amines in H-ZSM-5 plotted as a function of their proton-transfer energies in water. (Reprinted from ref 103. Copyright 1993 American Chemical Society.)

Table 3. Gas-Phase, Proton Affinities for Various Anions (kJ/mol)[a]

CH_3^-	1741	I^-	1312	NaOH	1036
$(CH_3)_3CO^-$	1554	HSO_4^-	1296	CsOH	1123
$(CF_3)_3CO^-$	1388	PO_3^-	1292	Na_2O	1375
CF_3COO^-	1351	$CF_3SO_3^-$	1280	Cs_2O	1442

[a] Data taken from refs 7 and 111–113. Data taken from ref 113 has been converted from free energies, assuming $\Delta S°$ is uniformly 22 cal/(mol K) for these acids.

ample, the value for ammonia is 858–145 kJ/mol.) Since PA_{ZO^-} is independent of the base, the linear correlation further requires that the intrazeolite ion pairing energy, c of the cycle, be identical for ammonium, methylammonium, dimethylammonium, ethylammonium, and isopropylammonium ions.

There are both theoretical and experimental estimates of the proton affinity of H-ZSM-5. Values range from 1160 kJ/mol[107] to 1374 kJ/mol.[108] From IR data, Datka has estimated a distribution of proton affinities corresponding to different Al–(OH)–Si sites of 1179–1333 kJ/mol.[22] If we take 1300 kJ/mol as representative of the range of suggested proton affinities, then we obtain 587 kJ/mol for $\Delta H_{interaction}$ for amines. Is this reasonable? A pure Coulomb attraction between point sources at 2.7 Å (the equilibrium separation between ZO^- and NH_4^+ calculated by van Santen et al.[109] would be worth 512 kJ/mol. Additional stabilization energy may come from hydrogen bonding[109] or long-range dielectric stabilization by the medium. Values that quantitatively define the cycle in Scheme 2, now emerging from a variety of sources, seem to be internally consistent; proton affinities are likely to be 1200–1350 kJ/mol and values for $\Delta H_{interaction}$ are likely to be 500–650 kJ/mol.

Let us look at the quantitative aspects to the cycle in a little more detail. How strong an acid is implied by a proton affinity of 1200 to 1350 kJ/mol? Gas-phase data for molecular acids are shown in Table 3. This is an interesting range in the gas-phase proton affinity scale. There have not been very many good experimental values in this range, although recent work of Koppel et al.[113] covers this range very thoroughly. It encompasses the low end of anion experimental data and the high end of the neutral data. For O–H acids, the high end of the zeolite proton affinity range is suggestive of strong carboxylic acids; the low end would appear to be stronger than trifluoromethanesulfonic acid. Anion proton affinities less than 1300 kJ/mol appear to imply substantial charge delocalization in the conjugate base, although Table 3 shows that it is possible to have a small molecular acid this strong where charge is delocalized over only a few atoms.

What is the nature of the interaction between the ammonium cations and the framework anions? It appears that a simple Coulomb, electrostatic, point-charge interaction would be adequate, if the proton affinity of the framework anion is at the low end of the suggested range. If additional interactions (H-bonding or dispersion interactions) are important, it would imply higher proton affinities. The binding energy/adsorbate proton-affinity correlation (Figure 6) shows a slope of one. Therefore, the change in the total binding energy of the adsorbate as the alkyl group is varied is fully accounted for by the corresponding change in the proton affinity of the amine. One might have expected any nonelectrostatic terms in the energy balance to be sensitive to substituent structure and destroy or reduce the slope of the correlation. For example, the strengths of gas-phase hydrogen bonds have been shown to scale with proton affinity.[106] Clearly, answering these types of questions will be possible with better theoretical and experimental values for the legs of this cycle.

Is it possible that H-ZSM-5 may contain a range of acid sites with proton affinities that differ by over 150 kJ/mol, as suggested by Datka et al.?[22] Can this be consistent with constant differential heats of adsorption for amine bases? Perhaps there are very strong compensation effects. That is, the conjugate bases of the high proton-affinity sites interact more strongly with the protonated amine, so that, as PA_{ZO^-} increases $\Delta H_{interaction}$ increases equivalently, allowing the binding energy, which is effectively the difference between these quantities, to remain constant. Certainly, one would expect this to occur to some extent. Weak acid sites (high PA_{ZO^-}) would have more charge-localized, conjugate bases that should be better hydrogen-bond acceptors. However, it is hard to see how one could get the perfect compensation implied by the constant differential heats, or the equivalent compensation for different amines implied by the slope of one. Perhaps the calorimetric measurement averages the different proton-affinity sites? Some averaging must occur because a temperature must be chosen where the adsorbate has some mobility. However, the range of proton affinities suggested by Datka is as large as the total binding energy. This is obviously an area that deserves more attention.

The two molecules that deviated from the linear correlation were *n*-butylamine and trimethylamine. In the case of *n*-butylamine, the adsorption enthalpy for the 1:1 complex is 15 kJ/mol higher than that which would be predicted by the straight-line relationship. Since the heats of adsorption for linear alkanes in silicalite are about 10 kJ/mol per C atom,[114] it seems plausible that the additional 15 kJ/mol for *n*-butylamine could be the result of dispersion forces between the alkyl group and the siliceous walls

of the zeolite channel. It is likely that smaller amines will now allow effective interactions between the alkyl group and the zeolite channels when the binding geometry is optimized to maximize the hydrogen-bonding interaction between the alkylammonium ion and the zeolite conjugate base. We suggest that the *n*-butyl group may extend far enough into the channel volume to regain part of the energy associated with the pure hydrocarbon adsorption in silicalite.

Trimethylamine is the other molecule which showed significant deviation from the line, falling approximately 20 kJ/mol below that predicted by the linear relationship. Two possible reasons for the lower than expected adsorption heats are as follows. First, it has been suggested that the formation of two or three hydrogen bonds between the NH_4^+ cation and the zeolite cluster is necessary to stabilize the intrazeolite ion pair complex.[109] With the exception of trimethylamine, all of the bases we have examined can form at least two hydrogen bonds to the zeolite matrix. Alternatively, the lower binding energy for trimethylamine may be the result of steric interactions which will not allow the large trimethylammonium ion to orient itself in the ZSM-5 channels in the optimum manner.

Similar, but less extensive adsorption calorimetry experiments have also been carried out on other high-silica zeolites, including H-ZSM-12, H-mordenite, and H-Y.[115] Again, most adsorbate/zeolite adsorption systems exhibited a constant heat of adsorption up to the coverage of one molecule per Brønsted acid site. Except for relatively small deviations which are probably due to specific interactions in particular adsorption systems, the enthalpies for ammonia, pyridine, and isopropylamine were within a few kilojoules/mole of 150, 200, and 210 kJ/mol for each of the zeolites. These values scale well with the gas-phase, proton affinities of the bases. Therefore, the sum of the vertical legs of the thermochemical cycle is not very sensitive to zeolite structure.

H-ZSM-5 has a much higher proton affinity than even the strongest adsorbate bases. The sum of the first two legs of the thermochemical cycle, that is, the hypothetical gas-phase proton transfer, is on the order of 400−500 kJ/mol endothermic for ammonia. Proton-transfer-induced chemisorption occurs because of the stabilization of the intrazeolitic ion pair. At some point, as the base strength of the adsorbate decreases, the interaction energy will be insufficient to overcome the proton transfer endothermicity. At this point, adsorption without proton transfer, a nonionic, probably hydrogen-bonded chemisorption mechanism, will prevail. It will be very interesting to determine where on the adsorbate basicity scale this point occurs for different functional groups. For example, acetone forms strong hydrogen bonds with Brønsted acid sites in H-ZSM-5 but NMR measurements indicate that the complete proton transfer does not occur.[98] In these types of systems, one may still expect the adsorption energies to scale with proton affinities, but the slope of the correlation should change.

Enthalpy Barriers to Alcohol and Thiol Decomposition

The thermochemical approach developed for amine adsorption is a step toward describing a potential energy surface for reactive systems. The solid acid-catalyzed reactions of simple alcohols and thiols have proven to be good probe reactions for expanding this approach to reactive adsorbates. In acidic solutions, alcohols are protonated to oxonium ions ($HROH_2^+$) which dehydrate to carbenium ions (HR^+) and water. The carbenium ion loses a proton to the medium to form the olefin (R). The corresponding mechanism in zeolites would be as shown:

$$HROH + ZOH = HROH_2^+ + ZO^- =$$
$$HR^+ + ZO^- + H_2O = R + H_2O + ZOH$$

mechanism 3

The reaction of thiols is completely analogous, proceeding through the intermediate sulfonium ion ($HRSH_2^+$):

$$HRSH + ZOH = HRSH_2^+ + ZO^- =$$
$$HR^+ + ZO^- + H_2S = R + H_2S + ZOH$$

mechanism 4

While these reactions do not have the commercial importance of hydrocarbon cracking or toluene alkylation, they are easier to understand and characterize. Stoichiometric adsorption complexes can be formed with most of the simple alcohols and thiols. Furthermore, because carbenium ions are important intermediates in many zeolite-catalyzed hydrocarbon reactions, the results have implications for understanding the more complex hydrocarbon reaction pathways as well.

For both alcohols and thiols, we have examined a series of adsorbate molecules that can form primary, secondary, and tertiary carbenium ions. In Figure 8, parts a−c, TPD-TGA curves are shown for ethanol, 2-propanol, and 2-methyl-2-propanol in H-ZSM-5. For ethanol, essentially all of the alcohol desorbs unreacted in two separate desorption events. The low-temperature feature at 370 K corresponds to bound molecules in excess of one/Al. These weakly adsorbed species can also be removed at room temperature by extended evacuation times. The high-temperature feature corresponds to a coverage of exactly one molecule per Al and is associated with molecules adsorbed at the Brønsted acid sites. With ethanol, the adsorption at the acid sites is reversible and the rate of desorption of ethanol from the acid sites is more rapid than dehydration.

For 2-propanol, the TGA trace is similar. Molecules in excess of a coverage of one/Al again desorb unreacted at lower temperatures. The 1:1 complex, however, reacts and desorbs as propene and water at ~405 K. Notice that the vacuum TGA experiment allows the unimolecular reactions that occur at the binding sites to be observed with minimal interference from secondary reactions of propene that complicate the chemistry under flowing gas conditions.[100] Because water and propene desorb simultaneously, the rate of product appearance in the vapor phase is limited by the reaction of the adsorbed 2-propanol, and not product diffusion. The reaction temperature is found to be independent of the Si/Al ratio of the H-ZSM-5 and is also the temperature at which 1:1

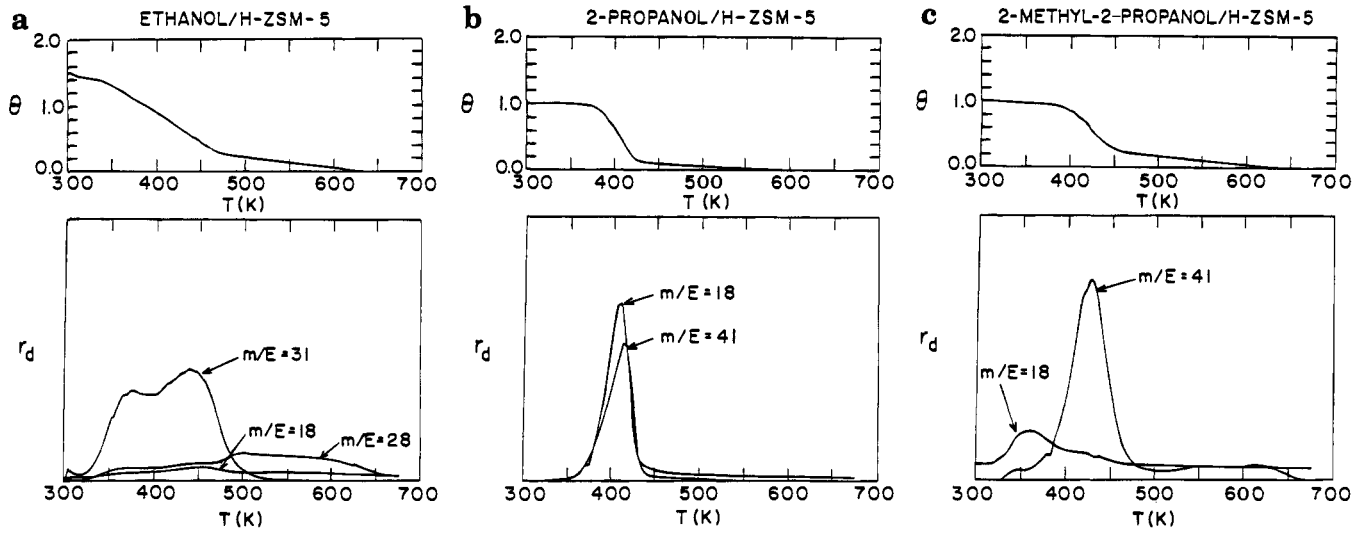

Figure 8. TPD-TGA curves for various alcohols in H-ZSM-5: (a) ethanol, (b) 2-propanol, and (c) 2-methyl-2-propanol. In these figures, the mass spectrometer signals are due to the following: ethanol (m/e = 31), water (m/e = 18), propene and other olefins (m/e = 41). (Reprinted from ref 100. Copyright 1986 Academic.)

Table 4. Calculated Energies for Mechanism 3 Based on Gas-Phase Proton Affinities (values in kJ/mol) (taken from ref 100)

HROH	HROH+ZOH	($HROH_2^+ZO^-$)	($HR^+ZO^-+H_2O$)	($R+ZOH+H_2O$)[a]
ethanol	0	−84	+75	+45.6
isopropyl alcohol	0	−88	−13	+51.0
tert-butyl alcohol	0	−105	−59	+52.7

[a] Calculated from standard heats of reaction.

adsorption complexes of 2-propanol react at the Brønsted acid sites of other high-silica zeolites.[116] Since TPD-TGA of 1-propanol is more similar to ethanol than to 2-propanol,[100] the high reactivity of 2-propanol is due to the lower formation energy of the secondary carbenium ion.

2-Methyl-2-propanol (*tert*-butyl alcohol) is much more reactive in these experiments than 2-propanol, as shown in Figure 8c). Following adsorption and evacuation, a coverage of close to one butanol molecule/Al is obtained. However, during TPD, no unreacted alcohol is observed. Water and a mixture of hydrocarbons are desorbed. The amount of water which desorbs during the temperature ramp is not enough to account for the amount of alcohol which has reacted. It appears that reaction occurs at room temperature and that most of the water desorbs during the evacuation period. The olefin products are a complex mixture implying that isobutene has undergone oligomerization and cracking reactions prior to leaving the sample. In fact, the products observed in desorption are essentially identical to those formed by the oligomerization and cracking of either ethene or propene in H-ZSM-5.[117]

We can treat these observations semiquantitatively using the thermochemical cycle (Scheme 2) and assuming mechanism 3 applies. We will take the sum of the vertical legs of the cycle to be 713 kJ/mol, as determined from calorimetry on amines (*vide infra*). This is, of course, a crude approximation since $\Delta H_{\text{Interaction}}$ must be sensitive to adsorbate structure. The assumption may not be too bad for alcohols since they are similar in size and hydrogen-bonding ability to the corresponding amines. It may be seriously wrong for the carbenium ions in the mechanism, however. Nevertheless, using this assumption, we may determine $\Delta H_{\text{binding}}$ for protonated alcohols from the alcohol gas-phase proton affinities and, for carbenium ions, from the corresponding olefin proton affinities. Some of the limitations of this approach have been discussed in detail elsewhere.[100,118] A table of the enthalpies of the various intermediates along the reaction coordinate estimated in this way are shown in Table 4.

The enthalpies in Table 4 do surprisingly well in rationalizing the experimental TPD-TGA data on alcohols. First, the model predicts that the heats of adsorption for the unreacted alcohols as oxonium ions should be in the range of 80 to 100 kJ/mol. This is consistent with desorption above room temperature and an estimate based on heats of immersion data.[119] Spectroscopic measurements for alcohol/H-ZSM-5 complexes, on the other hand, have been interpreted in terms of strong hydrogen bonding without proton transfer.[93] Indeed, calculations suggest that the neutral/neutral and cation/anion complexes are similar in free energy for alcohols.[110] If the oxonium ions are not the most stable structures of the alcohol complexes, they are at least readily kinetically accessible at room temperature. For example, HROD and ZOH undergo rapid isotope exchange at room temperature.[120] The model also clearly shows that the competition between dehydration and intact desorption should be controlled in large measure by the carbenium ion stability. For ethanol, starting with the adsorbed oxonium ion, one would predict the endothermicity for intact desorption would be 84 kJ/mol, compared to an endothermicity for dehydration of 75 to 84 = 159 kJ/mol. In this case, intact desorption should be favored. For 2-propanol, the predicted barriers for the two channels are close to equal, with dehydration being slightly favored (bar-

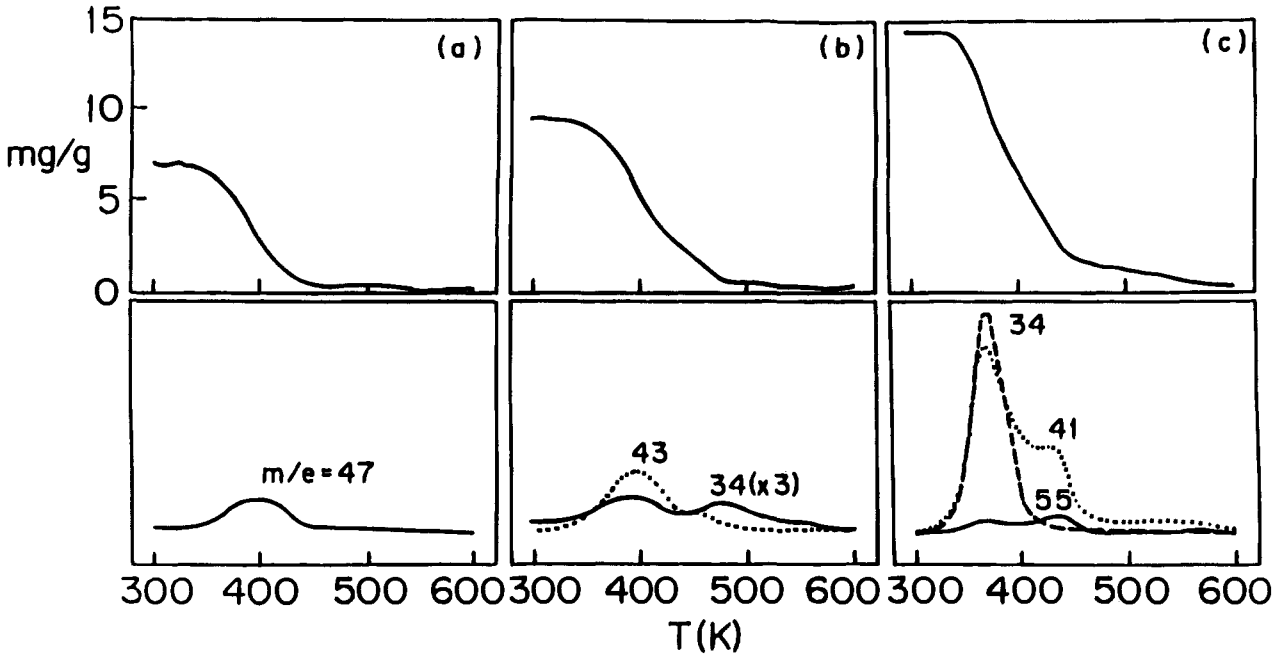

Figure 9. TPD-TGA curves for simple thiols in H-ZSM-12: (a) 1-propanethiol, (b) 2-propanethiol, and (c) 2-methyl-2-propanethiol. (Reprinted from ref 101. Copyright 1993 Butterworth.)

riers of 75 versus 88 kJ/mol). The observation that dehydration occurs during desorption, but not at room temperature, is in good agreement. The observation that propene and water from 2-propanol desorb at lower temperature than intact ethanol is also consistent. Finally, the predicted barrier for dehydration of *tert*-butyl alcohol is only 46 kJ/mol, which is low enough that one might expect dehydration rates to be substantial at room temperature, based on estimates from transition-state theory.[118]

Most of our work with thiols was carried out on H-ZSM-12 because 2-methyl-2-propanethiol was unable to enter the ZSM-5 pore structure and TPD-TGA results for alcohols and the smaller thiols were identical on H-ZSM-12,[101,116] For 2-methyl-2-propanethiol in H-ZSM-12, the observation of a stoichiometric complex was very clear. Molecules in excess of the 1:1 state desorbed rapidly during evacuation, while molecules associated with acid sites could not be removed at room temperature. It was possible to completely remove ethanethiol and 1-propanethiol from H-ZSM-12 with prolonged evacuation at room temperature; however, the affinity of the molecules for the Brønsted acid sites could be observed from measurements of the weight as a function of evacuation time at room temperature. During evacuation, the coverage rapidly leveled off at one/Al. Longer evacuation could reduce the coverage even further, but the rate of desorption from the 1:1 state was much slower.

The TPD-TGA curves for 1-propanethiol 2-propanethiol, and 2-methyl-2-propanethiol on H-ZSM-12 after 2 h evacuation are shown in Figure 9, parts a–c. For 1-propanethiol, desorption occurs from a single feature at ~390 K and no reaction products are observed. For 2-propanethiol, results show that most of this secondary thiol desorbs unreacted from a feature centered at ~400 K; however, a small amount of it reacts to propene and H_2S in the region of the high-temperature shoulder at ~470 K. Since most of the 2-propanethiol could be removed by prolonged evacuation at room temperature, we suggest that the molecules which react are not associated with a different type of acid site. Rather, during the TPD experiment, the temperature reaches the point at which decomposition rates compete with intact desorption before the adsorbate is completely removed. Apparently, the barrier for reaction of 2-propanethiol is only slightly higher than that for desorption. 2-Methyl-2-propanethiol on H-ZSM-12 could not be evacuated below a coverage of one/Al at room temperature, and the TPD-TGA curves demonstrate that all of the adsorbed thiol corresponding to this coverage reacts to H_2S and olefin products. In Figure 9c, all of the 2-methyl-1-propanethiol reacts in a peak at 380 K, where all of the H_2S and some of the olefin products leave the sample. While additional olefinic products are observed in the second feature at ~440 K, these are due to cracking of oligomerization products, similar to observations for *tert*-butyl alcohol.[100,117]

Using mechanism 4 and the same scheme discussed for alcohols, one can predict reactivities of simple thiols. The calculated enthalpies for the sulfonium ions and carbenium ions along the reaction coordinate are shown in Table 5. The proton affinities of simple thiols are slightly higher than the values for alcohols; and, therefore, the predicted heats of proton-transfer-induced adsorption for the thiols are higher. The fact that most of the thiols can be removed more readily by evacuation at room temperature indicates that the binding is, in fact, weaker. It is reasonable that $\Delta H_{\text{interaction}}$ derived for protonated amines overestimates thiol binding energies. The larger S atom should both increase the separation distance in the ion pair and decrease the hydrogen bond strength relative to amines.

Even so, the values in Table 5 still provide a reasonable explanation for the reactivity of the thiols. Because the reactions to form H_2S and the respective olefins from thiols are more endothermic than the analogous dehydration reactions for alcohols, the

Table 5. Potential Energy Diagram for the Thiol/Zeolite Interactions, Using HRSH + ZOH as a Reference (taken from ref 101)

	HRSH + ZOH	$HRSH_2^+ + ZO^-$	$HR^+ZO^- + H_2S$	$R + H_2S + ZOH$
ethyl	0	−100	105	78
n-propyl	0	−105	98	68
isopropyl	0	−109	13	76
tert-butyl	0	−121	−66	71

barrier for formation of the carbenium ions is increased significantly. Only for the 2-methyl-2-propanethiol is the decomposition predicted to be energetically favored, in good agreement with observations. Intact desorption of 2-propanethiol is predicted to be slightly favored over reaction, the reverse of 2-propanol. In accord with that prediction, intact desorption becomes the preferred desorption pathway from the thiol complex.

Olefin Oligomerization and Cracking

Reactions involving olefins (isomerization, oligomerization, alkylation, and cracking) are commercially very important. These reactions proceed through a classical, carbenium ion mechanism in Brønsted acids. In principle, the carbenium ion can be formed by adsorption of an olefin onto the protonic site, although it is likely that the ZO^-/carbenium ion pair is diverted to a covalently bound alkyl silyl ether as a more stable adsorbate structure.[120] The thermochemistry of the carbenium ion is still relevant, however, since the important chemistry must proceed through this intermediate. On the basis of the models described in the previous sections for amines, alcohols, and thiols, one can estimate the favorability of forming carbenium ions from the conjugate olefin bases if one again assumes $PA_{ZO^-} + \Delta H_{interaction}$ is 713 kJ/mol. As with thiols, there are good reasons to think that the carbenium ion/ZO^- anion heats of interaction calculated using this assumption will be too large. The simplest olefin, ethene, has a proton affinity of 686 kJ/mol. One predicts that adsorption to form the ethyl carbenium ion should be endothermic by 27 kJ/mol. In agreement with this, ethene at low pressures and temperatures remains only physisorbed in H-ZSM-5 and can be readily removed by evacuation.[117] Only by heating to above 370 K in the presence of ethene can one initiate reaction which results in the formation of oligomers in the zeolite.

On the other hand, propene, with a proton affinity of 775 kJ/mol, should form carbenium ions exothermically. It does react much more easily in H-ZSM-5, forming oligomers in the zeolite at room temperature and low pressures (<0.1 Torr). This is evidence that carbenium ions are formed in significant concentrations under these conditions, and that these intermediates react rapidly with unprotonated propene molecules to form oligomer chains. Reaction does not stop until a substantial fraction of the pore volume is filled. Additional evidence that relatively long hydrocarbon chains are formed by oligomerization of propene (or ethene at higher temperatures) is gained from ^{13}C NMR measurements, which indicate that the large majority of the carbons are part of saturated alkyl groups, with little evidence for olefinic or other types of carbon atoms.[118,121]

It is interesting to examine the thermal stability of the oligomers in H-ZSM-5. Figure 10 is the typical

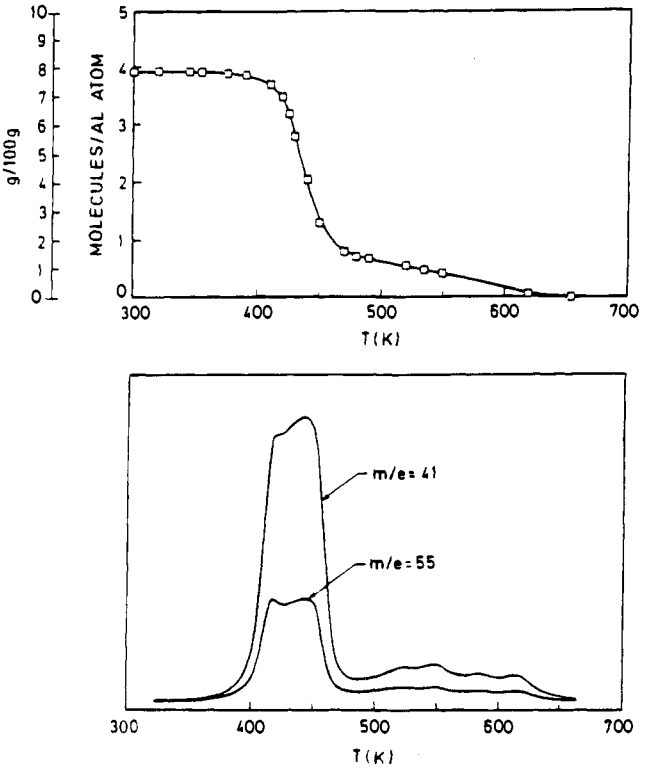

Figure 10. TPD-TGA curves for H-ZSM-5 following exposure to 15 Torr of propene at room temperature. The peak at $m/e = 55$ indicates that olefins larger than propene are desorbing from the sample. (Reprinted from ref 117. Copyright 1989 Academic.)

TPD-TGA result obtained for a sample following exposure to 10 Torr of propene for 15 min. The initial coverage, 80 mg per gram of catalyst, corresponds to ~4 molecules of propene/Al site. Cracking of the oligomers begins above 400 K and most of the hydrocarbons have been removed by ~500 K in this particular sample, although the final reaction temperature appears to depend on the starting olefin and the sample history.[23,117] The peaks at $m/e = 41$ and 55 in the mass spectrum of the desorbing species are common to many olefins, although the peak at 55 shows that at least some of the products have molecular weights greater than that of propene. A more careful analysis, performed by trapping the products and analyzing them using a gas chromatograph, indicates that the desorbing species ranged from ethene to C-7 hydrocarbons, with no preference for propene or hexenes. Due to the large number of isomers observed in the chromatogram, it was not possible to analyze the products in detail. This would probably depend on the sample characteristics and experimental apparatus; however, the relative concentration of the four butenes, isobutene, 1-butene, and *cis*- and *trans*-2-butene, are present in their equilibrium concentrations, implying that thermodynamic, rather than kinetic, properties dictate the product distribution.

The results described above provide important insights into some of the chemistry of olefins in zeolites. For example, it appears that a substantial fraction of the pore volume of the zeolite is likely to be filled with oligomer chains when olefin reactions are carried out at temperatures below 400−500 K.[58,117] Low-temperature reaction studies have been shown to produce isomerization[122] or dimer and trimer products rather than the more complex mixture obtained by cracking of the adsorbed oligomers. The chemisorption studies suggest that these isomerization reactions of olefins at low temperatures may be due to reaction on the external surface of the zeolite, since the large majority of the acid sites should be poisoned by oligomer chains. Reaction rates and products may not be representative of the majority of sites. At higher temperatures, it seems reasonable that the growing and cracking of chains are competing processes which lead to the wide product distributions that are observed.

Spectroscopic Investigations of Adsorbed Intermediates

In the above sections, we have used gas-phase data as the basis for rationalizing the chemistry and thermochemistry of simple amines, alcohols, thiols, and olefins in H-ZSM-5. While this gas-phase model has been very helpful for understanding many aspects of the Brønsted acid site chemistry, there have been some significant discrepancies. Two examples are as follows: (1) The heat of adsorption for *n*-butylamine is greater than predicted and the heat of trimethylamine less than predicted by the model; and (2) thiols, which have a higher proton affinity than alcohols, can be evacuated much more readily after adsorption at the Brønsted acid sites than alcohols. As stated in earlier sections, these deviations and others suggest specific situations where the assumptions of the model are inadequate. The calculations of adsorption complex stabilities have assumed the following: (1) There is complete proton transfer from the acid site to the adsorbed intermediate to form an ion-pair complex, and (2) the bonding between the cationic adsorbate and the framework anion is not sensitive to the detailed structure of the cation, where alkylammonium ions provide the thermochemical standard. One can say that, in studying the breakdown of these assumptions, one is studying the nature of specific interactions between the adsorbate and the lattice during proton transfer in the zeolite. A better picture of zeolite acidity with improved capability for predicting reactivity requires a more detailed picture of the interactions within the adsorption complexes. In particular, ^{13}C NMR of the 1:1 complexes has been shown to be very informative in filling in the details of this picture.

In this section, we will describe the ^{13}C NMR spectra of three types of intermediates. First, we will briefly discuss a few examples where the intermediates appear to be truly ionic and display spectral properties that are similar to those observed in superacid solutions. Second, we will describe adsorption complexes where the interaction seems to be best described as dominated by strong hydrogen bonding. There is a gradation in the extent of proton transfer that occurs in these complexes which may be related to differences in the proton affinities of the adsorbate molecules. (For example, in a comparison of acetone and mesityl oxide, proton transfer is much more extensive with mesityl oxide.) Finally, we describe "carbenium ions" formed by the dehydration of *tert*-butyl alcohol or the protonation of olefins.

It is worth repeating that our work was greatly simplified by the observation that well-defined adsorption complexes can be formed by many molecules with the protonic sites in high-silica zeolites. By monitoring the reaction chemistry and stoichiometries in separate TPD-TGA and IR experiments, spectroscopic assignments could be verified.

Ionic Adsorption Complexes

There are a number of examples where the adsorption complexes can be described as ionic, including pyridine,[72] and simple amines. One of the nicest examples of an important, ionic reaction intermediate is the formation of imonium ions from the nucleophilic attack of adsorbed aldehydes by added ammonia.[96] The NMR spectra of these intermediates are essentially identical to the corresponding spectra in magic acids. This work is discussed in detail elsewhere;[33] and we simply note that the molecules which are completely protonated by the zeolite, such as imines, are all strong gas-phase bases (proton affinity > ammonia).

Hydrogen-Bonded Complexes

For some molecules, proton transfer is not complete and the adsorption complex is probably best described as being hydrogen bonded. While there is no clear demarcation between ionic and hydrogen-bonded complexes, some molecules complexed to strong Brønsted sites are not adequately described as being protonated, either in the zeolite or in solution. For example, Maciel and Natterstad demonstrated that the isotropic chemical shifts for the carbonyl carbon of acetone in different acid solutions follow a regular relationship between the magnitude of the chemical shift and the strength of the acid. For acetone in formic acid (pK_a = 3.75), dichloroacetic acid (pK_a = 1.26), trifluoroacetic acid (pK_a = 0.23), and sulfuric acid (pK_a = 5.2), the chemical shifts were 9.1, 11.9, 14.1, and 39.2 ppm respectively from neat acetone.[123] In media which were nonprotonic but varied significantly in polarity, the chemical shifts deviated negligibly from that of pure acetone, indicating that the differences in chemical shift for acetone in protic solutions are due to hydrogen bonding between the acids and the carbonyl group. Only in the case of sulfuric acid could the acetone be considered to be "protonated". In the other acids, rapid equilibrium between the keto and enol forms of acetone, or between the protonated and unprotonated species, could be ruled out as explanations for the observed chemical shift. Theoretical considerations confirm that the chemical shift for the carbonyl carbon should be affected by the strength of the hydrogen bond.[124]

In H-ZSM-5 at low coverages (below one/Al), acetone molecules remain unreacted below 400 K and are localized at the acidic hydroxyls, as demonstrated in the section on stoichiometric adsorption complexes. The isotropic chemical shift for the carbonyl carbon

at 125 K is significantly shifted from neat acetone. As in solution, the shift can be interpreted as a measure of the ability of the site to form a hydrogen bond with the carbonyl oxygen and, therefore, should be related to the intrinsic acidity of the site. For all coverages below one/Al site, there is a single isotropic chemical shift, centered at ~17 ppm from the neat acetone, indicating that all sites are virtually identical in their ability to form hydrogen bonds. Because the molecules are localized at the sites and the isotropic chemical shift does not change with temperature, the interaction between acetone and the acid sites must involve hydrogen bonds and not any equilibrium process, just as in the solution case.

For the same reasons that pK_a is not a good scale for comparing solid acid/base interactions in calorimetry, it is not particularly meaningful to assign a pK_a value for H-ZSM-5 from the acetone chemical shift. However, because the solution chemical shift data seems to reflect a relatively pure proton-donor effect for acetone and may be more or less sensitive to polarity effects for other probe molecules, varying the probe molecule may be a technique to separate hydrogen-bond strength and dielectric stabilization effects in the zeolite pore.

Mesityl oxide is another example of a molecule which forms a strongly hydrogen-bonded complex in H-ZSM-5. Because the protonated form of this molecule is resonance stabilized, significant portions of the charge are localized on both the carbonyl carbon and the β carbon, resulting in large ^{13}C isotropic chemical shifts for both carbons, from 195.9 to 215.5 ppm for the carbonyl carbon and from 152.5 to 181.8 ppm for the β carbon in magic acids.[125] In H-ZSM-5, the molecules at the Brønsted-acid sites exhibit chemical shifts of 210 and 188 ppm for the carbonyl carbon and the β carbon respectively.[33] Again, the molecule at the acid sites is rigid and the observed chemical shifts cannot be due to a chemical equilibrium between a protonated and unprotonated species. The fact that the chemical shifts for mesityl oxide in the adsorption complex are close, but not identical, to that found in the magic acids suggests that there is almost complete proton transfer from the site to the adsorbate. The fairly large difference in the magnitude of the β carbon shift can probably be interpreted in terms of the differences between the way the hydrogen-bound ketone interacts with either the solvent or the zeolite framework.

Olefins and tert-Butyl Alcohol

As we described in an earlier section, the structure of olefin/zeolite adsorption complexes is of great interest. However, investigations of "adsorbed" olefins are very difficult due to the fact that olefins oligomerize rapidly at zeolite acid sites, so that the intermediates cannot be unambiguously identified. (See, for example, the discussion of spectroscopic data in refs 117 and 100.) The formation of a carbenium ion-like intermediate can be controlled more easily starting with the *tert*-butyl alcohol. TPD-TGA studies demonstrate that this alcohol reacts at room temperature and that the water formed in the reaction can be removed by evacuation. The species remaining in the zeolite has similar properties to adsorbed olefins and many of the properties one might expect of a carbenium ion, including the following: (1) The species exists at a stoichiometry close to one/Al. (2) The species is present at the Al site, as evidenced by the fact that the 3605-cm^{-1} hydroxyl associated with the acid sites is absent.[120] (3) The intermediate undergoes rapid H/D exchange at room temperature when exposed to D_2O, forming C−D bonds at the expense of C−H bonds.[120] (4) The complex is highly reactive, undergoing chemistry similar to that which would be expected for a carbenium ion.[117]

To characterize the structure of this complex, 95% ^{13}C-enriched $(CH_3)_3{}^{13}COH$ was adsorbed onto an H-ZSM-5 sample.[118] Due to the high reactivity of the alcohol in the presence of H-ZSM-5, the spectroscopic features were found to depend on the sample preparation techniques. For adsorption onto a 150-mg sample in a packed tube, oligomerization products dominated the spectrum. Apparently, adsorption onto a "deep" catalyst bed resulted in nonuniform adsorbate coverages with significant local concentration of neutral olefins near Brønsted sites. Following dehydration, the olefins in these "deep-bed" samples rapidly oligomerized. Oligomerization could be minimized by spreading the zeolite over a larger area, although secondary reactions were still observed.

The magic-angle-spinning (MAS), ^{13}C NMR spectra of the 1:1 adsorption complex, prepared in a manner identical to that used in the TPD-TGA experiments, exhibit two large peaks at 29.4 (saturated alkyl groups) and 77.6 ppm (carbon covalently bonded to oxygen) relative to TMS, along with a small feature at 123 ppm (olefinic carbons). No spectral features near 330 ppm, which could be assigned to a *tert*-butyl carbenium ion based on superacid solution precedents, were observed. Since TPD-TGA results indicate that dehydration and subsequent water desorption have occurred prior to the NMR measurements, the presence of covalent carbon−oxygen bond implies that an alkoxy, or alkylsilyl ether intermediate must have formed. Furthermore, since the initial alcohol was labeled only at the hydroxyl carbon, the presence of ^{13}C-labeled aliphatic carbon atoms indicates that additional reaction has occurred which scrambles the label. Some of this transformation was due to oligomerization reactions. The alkoxy species loses a proton to the zeolite to form the olefin, which can then migrate and react with a dehydrated alcohol complex at an adjacent site. This was verified by heating the sample in the sealed rotor, after which the 29.4-ppm peak increased at the expense of the 77.6-ppm peak. However, the spectrum suggests that there is an additional scrambing mechanism, perhaps the result of intramolecular hydride and alkyl shifts. Simple oligomerization of 2-^{13}C-methylpropene should result in a product in which all of the carbon atoms are in tertiary positions. The peak width and structure of the alkyl carbon signal suggests that the label is more completely scrambled.

It is relatively easy to understand why the spectroscopically observed intermediate is the alkylsilyl ether, rather than the carbenium ion. In solution, long-lived carbenium ions are observed only in nonnucleophilic, high dielectric constant media. Unless the framework anion is highly delocalized, the conjugate base of the zeolite Brønsted site will hardly

be nonnucleophilic. Earlier in this article, we presented arguments that the anion is not highly delocalized. (On the basis of H/D exchange experiments and transition state theory, one can estimate the bound, tertiary carbenium ion to be less stable than the silyl ether by ~20 kJ/mol.[118]) The large reactivity differences observed for the various alcohols (*vide infra*) imply that reactions occur through the carbocation.

For more complex olefins which typically have higher proton affinities, the additional stabilities seem to be enough to tip the balance in favor of the carbenium ion.[121] One of the really interesting questions in this field is how to determine when this crossover from alkoxide to carbenium ion occurs.

Conclusions

Our goal in this paper has been to describe progress toward a description of acid-catalyzed reactions in zeolites based on realistic potential surfaces. The first step in this direction is to clarify the distinction between acidity, an equilibrium thermodynamic concept, and activity, a composite kinetic concept. We have shown how gas-phase proton affinities of reference bases can be used within a thermochemical cycle to separate the overall thermochemistry of adsorbate binding at zeolite Brønsted sites into two terms: (1) an intrinsic zeolite proton affinity, and (2) an interaction enthalpy that results from allowing the conjugate base of the zeolite and the conjugate acid of the adsorbate to relax into an equilibrium structure. This is a thermochemical picture built around the local structural features of zeolite Brønsted sites. All of the experimental techniques that have traditionally been used to probe proton transfer in zeolites have important contributions to make toward the elaboration of this picture. The powerful combination of *ab initio* quantum-mechanical calculations with calorimetry, TPD, NMR, and IR is already leading to new insights into the driving forces for intrazeolite reactions. We believe the day is not far off when it will be possible to talk about structure/activity relationships among acidic zeolites in terms of well-defined thermochemical quantities like proton affinities and adsorbate reorientation energies.

Acknowledgments

The authors acknowledge support from the National Science Foundation. Many of the ideas in this paper were developed in collaboration with other colleagues, especially Professors David White and George Kokotailo, and students Mike Grady, Mark Aronson, Tammy Kofke, Candido Pereira, Andy Biaglow, Dave Parrillo, Jelena Sepa, and Chi Lee. We also thank Willis Dolinger and Erik Thiele for their assistance in obtaining some of the data described in this paper.

References

(1) These distinctions are discussed in detail: Gilespie, R. J. *Proton-Transfer Reactions*; Caldin, E. F.; Gold, V., Ed.; Chapman and Hall: London, 1975; pp 1–30.
(2) Brønsted, J. *Rec. Tran. Chim.* **1923**, *42*, 718.
(3) Arnett, E. M. *Proton Transfer Reactions*; Caldin, E. F., Gold, V., Eds.; Chapman and Hall: London, 1975; p 88.
(4) Fleischer, U.; Kutzellnig, W.; Bleiber, A.; Sauer, J. *J. Am. Chem. Soc.* **1993**, *115*, 7833.
(5) Teunissen, E. H.; van Duijneveldt, F. B.; van Santen, R. A. *J. Phys. Chem.* **1992**, *96*, 366.
(6) Aue, D. H.; Bowers, M. T. *Gas Phase Ion Chemistry*, *2*; Academic Press: New York, 1979; p 1.
(7) Lias, S. G.; Bartmess, J. E.; Liebman, J. F.; Holmes, J. L.; Levin, D. R.; Mallard, G. W. *J. Phys. Chem. Ref. Data* **1988**, *17*, Suppliment 1, and references therein.
(8) Wolf, J. F.; Harch, P. G.; Taft, R. W. *J. Am. Chem. Soc.* **1975**, *97*, 2906.
(9) Sauer, J. *Chem. Rev.* **1989**, *89*, 199.
(10) Parrillo, D. J.; Lee, C.; Gorte, R. J. *Appl. Catal., A* **1994**, *110*, 67.
(11) Parry, E. P. *J. Catal.* **1963**, *2*, 371.
(12) Emeis, C. A. *J. Catal.* **1993**, *141*, 347.
(13) Zholobenko, V. L.; Makarova, M. A.; Dwyer, J. *J. Phys. Chem.* **1993**, *97*, 5962.
(14) Karge, H. G. *Catalysis and Adsorption by Zeolites*; Ohlmann et al., Eds.; Elsevier: Amsterdam, 1991; p 133.
(15) Pelmenshchikov, A. G.; Paukshtis, E. A.; Stepanov, V. G.; Pavlov, V. I.; Yurchenko, E. N.; Ione, K. G.; Beran, S. *J. Phys. Chem.* **1989**, *93*, 6725.
(16) Schröder, K.-P.; Sauer, J.; Leslie, M.; Catlow, C. R. A.; Thomas, J. M. *Chem Phys Lett.* **1992**, *188*, 320.
(17) Brand, H. V.; Curtiss, L. A.; Iton, L. E. *J. Phys. Chem.* **1992**, *96*, 7725.
(18) Jacobs, P. A.; von Ballmoos, R. *J. Phys. Chem.* **1982**, *86*, 3050.
(19) Ison, A.; Gorte, R. J. *J. Catal.* **1984**, *89*, 150.
(20) Woolery, G. L.; Alemany, L. B.; Dessau, R. M.; Chester, A. W. *Zeolites* **1986**, *6*, 14.
(21) Dessau, R. M.; Schmitt, K. D.; Kerr, G. T.; Woolery, G. L.; Alemany, L. B. *J. Catal.* **1987**, *104*, 484.
(22) Datka, J.; Boczar, M.; Gil, B. *Langmuir* **1993**, *9*, 2496.
(23) Grady, M. C.; Gorte, R. J. *J. Phys. Chem.* **1985**, *89*, 1305.
(24) Farneth, W. E.; Roe, D. C.; Kofke, T. J. G.; Tabak, C. J.; Gorte, R. J. *Langmuir*, **1988**, *4*, 152.
(25) Biaglow, A. I.; Parrillo, D. J.; Gorte, R. J. *J. Catal.* **1993**, *144*, 193.
(26) Fritz, P. O.; Lunsford, J. H. *J. Catal.* **1989**, *118*, 85.
(27) Martens, J. A.; Jacobs, P. A. *Zeolites* **1986**, *6*, 334.
(28) Bourdillon, G.; Gueguen, C.; Guisnet, M. *Appl. Catal.* **1990**, *61*, 123.
(29) Ashton, A. G.; Batmanian, S.; Clar, D. M.; Dwyer, J.; Fitch, F. R.; Hinchcliffe, A.; Machado, F. J. *Catalysis by Acids and Bases*; Imelik, B., Ed.; Elsevier: Amsterdam, 1985; p 101.
(30) Barthomeuf, D. *Catalysis by Acids and Bases*, Imelik, B., Ed.; Elsevier: Amsterdam, 1985; p 75.
(31) Bosacek, V.; Kubelkova, L.; Novakova, J. *Stud. Surf. Sci. Catal.* **1991**, *65*, 337.
(32) Munson, E. J.; Haw, J. F. *Angew. Chem., Int. Ed. Engl.* **1993**, *32*, 615.
(33) Biaglow, A. I.; Sepa, J.; Gorte, R. J.; White, D. *J. Catal.* **1995**, *151*, 373.
(34) Ward, J. W. *J. Catal.* **1968**, *11*, 259.
(35) Abott, J.; Guerzoni, F. N. *Appl. Catal.* **1992**, *85*, 173.
(36) Gates, B. C.; Katzer, J. R.; Schuit, G. C. A. *Chemistry of Catalytic Processes*; McGraw-Hill: New York, 1979; p 14.
(37) Haag, W. O.; Dessau, R. M. *Proc. Int. Congr. Catal.* **1984**, *305* (Vol. 2, Berlin).
(38) McVicker, G. B.; Kramer, G. M.; Ziemiak, J. J. *J. Catal.* **1983**, *83*, 286.
(39) Krannila, H.; Haag, W. O.; Gates, B. C. *J. Catal.* **1992**, *135*, 115.
(40) Mota, C. J. A.; Nogueira, L.; Kover, W. B. *J. Am. Chem. Soc.* **1992**, *114*, 1121.
(41) Poutsma, M. L. *ACS Monograph* **1976**, *171*, 437.
(42) Fripiat, J. G.; Berger-Andre, F.; Andre, J. M.; Derouane, E. G. *Zeolites* **1983**, *3*, 306.
(43) Derouane, E. G. In *Guidelines for Mastering the Properties of Molecular Sieves*; Barthomeuf, D., et al., Eds.; Plenum Publishing Co.: New York, 1990; p 234.
(44) Lombardo, E. A.; Hall, W. K. *J. Catal.* **1988**, *112*, 565.
(45) Lombardo, E. A.; Pierantozzi, R.; Hall, W. K. *J. Catal.* **1988**, *110*, 171.
(46) Beynon, J. H.; Gilbert, J. R. *Gas-Phase Ion Chemistry*; Bowers, M. T., Ed.; Academic Press: New York, 1979; Vol. 2, p 153.
(47) Beaumont, R.; Barthomeuf, D. *J. Catal.* **1972**, *26*, 218.
(48) Mikovksy, R. J.; Marshall, J. F. *J. Catal.* **1976**, *44*, 170.
(49) Mortier, W. J. *J. Catal.* **1978**, *55*, 138.
(50) Prins, R. Private communication, 1994.
(51) Haag, W. O.; Chen, N. Y. In *Catalyst Design: Progress and Perspectives*; Hegedus, L. L., Ed.; Wiley: New York, 1987; p 180.
(52) DeCanio, S. J.; Sohn, J. R.; Fritz, P. O.; Lunsford, J. H. *J. Catal.* **1986**, *101*, 132.
(53) Fyfe, C. A.; Gobbi, G. C.; Klinowski, J.; Thomas, J. M.; Ramdas, S. *Nature* **1982**, *296*, 530.
(54) Lombardo, E. A.; Sill, G. A.; Hall, W. K. *J. Catal.* **1989**, *119*, 426.
(55) Beyerlein, R. A.; McVicker, G. B.; Yacullo, L. N.; Ziemiak, J. J. *J. Phys. Chem.* **1988**, *92*, 1967.

(56) Lago, R. M.; Haag, W. O.; Mikovsky, R. J.; Olson, D. H.; Hellring, S. D.; Schmitt, K. D.; Kerr, G. T. In *Proceedings, 7th International Zeolite Conference*; Murakami, Y., Iijima, A., Ward, J. W., Eds.; Kodansha Ltd.: Tokyo, 1986; p 677.
(57) Lonyi, F.; Lunsford, J. H. *J. Catal.* **1992**, *136*, 566.
(58) Biaglow, A. I.; Parrillo, D. J.; Kokotailo, G. T.; Gorte, R. J. *J. Catal.* **1994**, *148*, 213.
(59) Zholobenko, V. L.; Kustov, L. M.; Borovkov, V. Y.; *Kazanskii. Kinet. Katal.* **1987**, *28*, 965.
(60) Walling, C. *J. Am. Chem. Soc.* **1950**, *72*, 1164.
(61) Tanabe, K. *Solid Acids and Bases*; Academic Press: New York, 1970.
(62) Atkinson, D.; Curthoys, G. *Chem. Soc. Rev.* **1979**, *8*, 475.
(63) Umansky, B. S.; Hall, W. K. *J. Catal.* **1990**, *124*, 97.
(64) Arnett, E. M.; Haaksma, R. A.; Chawla, B.; Healy, M. H. *J. Am. Chem. Soc.* **1986**, *108*, 4888.
(65) Farcasiu, D.; Ghenciu, A. *J. Am. Chem. Soc.* **1993**, *115*, 10901.
(66) Kiriesi, I.; Forster, H.; Tasi, G.; Fejes, P. In *Catalysis and Adsorption by Zeolites*; Ohlmann, G., et al., Eds.; Elsevier: Amsterdam, 1991.
(67) Vedrine, J. C. In *Guidelines for Mastering the Properties of Molecular Sieves*; Bartomeuf, D., et al., Eds.; Plenum: New York, 1990.
(68) Anderson, J. R.; Foger, K.; Mole, T.; Rajadhyakshan, R. A.; Sanders, J. V. *J. Catal.* **1979**, *58*, 114.
(69) Nayak, V. S.; Choudhary, V. R. *J. Catal.* **1983**, *81*, 26.
(70) Demmin, R. A.; Gorte, R. J. *J. Catal.* **1984**, *90*, 32.
(71) Sharma, S. B.; Meyers, B. L.; Chen, D. T.; Miller, J.; Dumesic, J. A. *Appl. Catal. A*, **1993**, *102*, 253.
(72) Parrillo, D. J.; Adamo, A. T.; Kokotailo, G. T.; Gorte, R. J. *Appl. Catal.* **1990**, *67*, 107.
(73) Malysheva, L. V.; Paukshtis, E. A.; Katarenko, N. S. *J. Catal.* **1987**, *104*, 31.
(74) Juskelis, M. V.; Slanga, J. P.; Roberi, T. G.; Peters, A. W. *J. Catal.* **1992**, *138*, 391.
(75) Kofke, T. J.; Gorte, R. J.; Kokotailo, G. T. *J. Catal.* **1989**, *116*, 252.
(76) Kofke, T. J.; Gorte, R. J.; Kokotailo, G. T. *Appl. Catal.* **1989**, *54*, 177.
(77) Tittensor, J. G.; Gorte, R. J.; Chapman, D. M. *J. Catal.* **1992**, *138*, 714.
(78) Biaglow, A. I.; Gittleman, C.; Gorte, R. J.; Madon, R. J. *J. Catal.* **1991**, *129*, 88.
(79) Pereira, C.; Gorte, R. J. *Appl. Catal.* **1992**, *90*, 1.
(80) Cardona-Martinez, N.; Dumesic, J. A. *Adv. Catal.* **1992**, *38*, 149.
(81) Auroux, A.; Vedrine, J. C. *Stud. Surf. Sci. Catal.* **1985**, *20*, 311.
(82) Auroux, A.; Ben Taarit, Y. *Thermochem. Acta* **1987**, *122*, 63.
(83) Chen, D. T.; Sharma, S. B.; Cardona-Martinez, N.; Dumesic, J. A.; Bell, V. A.; Hodge, G. D.; Madon, R. J. *J. Catal.* **1992**, *136*, 392.
(84) Gonzalez, M. R.; Sharma, S. B.; Chen, D. T.; Dumesic, J. A. *Catal. Lett.* **1993**, *18*, 183.
(85) Chen, D. T.; Sharma, S. B.; Filimonov, I.; Dumesic, J. A. *Catal. Lett.* **1992**, *12*, 201.
(86) Klinowski, J. *Chem. Rev.* **1991**, *91*, 1459.
(87) Kenaston, N. P.; Bell, A. T.; Reimer, J. A. *J. Phys. Chem.* **1994**, *98*, 894.
(88) Gil, B.; Browclawik, E.; Datka, J.; Klinowski, J. *J. Phys. Chem.* **1994**, *98*, 930.
(89) Pfiefer, H.; Freude, D.; Kärger, J. *Catalysis and Adsorption by Zeolites*; Ohlmann et al., Eds.; Elsevier: Amsterdam, 1991.
(90) Hunger, M.; Freude, D.; Fenzke, D.; Pfeifer, H. *Chem. Phys. Lett.* **1992**, *191*, 391.
(91) Gluszak, T. J.; Chen, D. T.; Sharma, S. B.; Dumesic, J. A.; Root, T. W. *Chem. Phys. Lett.* **1992**, *190*, 36.
(92) Batamack, P.; Doremieux-Morin, C.; Fraissard, J. *J. Chim. Phys.* **1992**, *89*, 423.
(93) Aronson, M. T.; Gorte, R. J.; White, D.; Farneth, W. E. *Langmuir* **1988**, *4*, 702.
(94) Anderson, M. W.; Klinowski, J. *Nature* **1989**, *339*, 200.
(95) Tsiao, C.; Corbin, D. R.; Dybowski, C. *J. Am. Chem. Soc.* **1990**, *112*, 7140.
(96) Bosacek, V.; Kubelkova, L.; Kovakova, J. *Stud. Surf. Sci. Catal.* **1991**, *65*, 337.
(97) Xu, T.; Munson, E. J.; Haw, J. F. *J. Am. Chem. Soc.* **1994**, *116*, 1962.
(98) Biaglow, A. I.; Gorte, R. J.; White, D. *J. Catal.* **1994**, *148*, 779.
(99) Kofke, T. J. G.; Gorte, R. J.; Farneth, W. E. *J. Catal.* **1988**, *114*, 34.
(100) Aronson, M. T.; Gorte, R. J.; Farneth, W. E. *J. Catal.* **1986**, *98*, 434.
(101) Pereira, C.; Gorte, R. J.; Kokotailo, G. T. *Proceedings from the Ninth International Zeolite Conference, Vol. 2*; von Ballmoos, R., et al., Eds.; Butterworth: Amsterdam, 1993; p 243.
(102) Biaglow, A. I.; Gorte, R. J.; White, D. *J. Phys. Chem.* **1993**, *97*, 7135.
(103) Parrillo, D. J.; Gorte, R. J.; Farneth, W. E. *J. Am. Chem. Soc.* **1993**, *115*, 12441.
(104) Reichardt, C. *Solvents and Solvent Effects in Organic Chemistry*, 2nd ed.; VCH: Weinheim, 1990; p 20.
(105) Similar observations have been reported: Pankrahev, Y. D.; Paukshtis, E. A.; Turkov, V. M.; Yurchenko, E. N. *Acta. Phys. Chem.* **1985**, *31*, 55.
(106) Moet-Ner, M. *J. Phys. Chem.* **1987**, *91*, 417.
(107) Brand, H. V.; Curtiss, L. A.; Iton, L. E. *J. Phys. Chem.* **1992**, *96*, 7725.
(108) Kramer, G. J.; van Santen, R. A. *J. Am. Chem. Soc.* **1993**, *115*, 2887.
(109) Teunissen, E. H.; van Santen, R. A.; Jansen, A. P. J.; van Duijneveldt, F. B. *J. Phys. Chem.* **1993**, *97*, 203.
(110) For example, the neutral, H-bonded complex for methanol at a Brønsted site is estimated to be only 12kJ/mol more stable than the oxonium-ion pair: Sauer, J. *Stud. Surf. Sci. Catal.* **1994**, *84*, 2039.
(111) Gal, J. F.; Mariua, P. C. *Prog. Phys. Org. Chem.* **1990**, *17*, 159.
(112) Bartmess, J. E.; McIver, R. T. *Gas Phase Ion Chemistry*; Bowers, M. T., Ed.; Academic Press: New York, 1979; Vol. 2, p 88.
(113) Koppel, I. A.; Taft, R. W.; Anvia, F.; Zhu, S.-Z.; Hu, L.-Q.; Sung, K.-S.; Des Marteau, D. D.; Yagupolskii, L. M.; Yagupolskii, Y. L.; Ignat'ev, N. V.; Kondratenko, N. V.; Volkonskii, A. U.; Vlasov, V. M.; Notario, R.; Maria, P.-C. *J. Am. Chem. Soc.* **1994**, *116*, 3047.
(114) Rees, L. V. C.; Hampson, J.; Brückner, P. *Zeolites Microporous Solids: Synthesis, Structure, and Reactivity*; Derouane, E. G., et al., Eds.; Kluwer Academic Publishers: Netherlands, 1992; p 133.
(115) Parrillo, D. J.; Gorte, R. J. *J. Phys. Chem.* **1993**, *97*, 8786.
(116) Kofke, T. J. G.; Gorte, R. J.; Kokotailo, G. T.; Farneth, W. E. *J. Catal.* **1989**, *115*, 265.
(117) Kofke, T. J. G.; Gorte, R. J. *J. Catal.* **1989**, *115*, 233.
(118) Aronson, M. T.; Gorte, R. J.; Farneth, W. E.; White, D. *J. Am. Chem. Soc.* **1989**, *111*, 840.
(119) Messow, U.; Quitzsch, K.; Herden, H. *Zeolites* **1984**, *4*, 255.
(120) Aronson, M. T.; Gorte, R. J.; Farneth, W. E. *J. Catal.* **1987**, *105*, 455.
(121) van den Berg, J. P.; Wolthuizen, J. P.; Clague, A. D. H.; Hays, G. R.; Huis, R.; van Hooff, J. H. C. *J. Catal.* **1983**, *80*, 130.
(122) Kramer, G. M.; McVicker, G. B.; Ziemiak, J. J. *J. Catal.* **1985**, *92*, 355.
(123) Maciel, G. E.; Natterstad, J. J. *J. Chem. Phys.* **1965**, *42*, 2752.
(124) White, D.; Evleth, E.; Kassab, V.; Allevena, M. Unpublished calculations.
(125) Olah, G. A.; Halpern, Y.; Mo, Y. K.; Lang, G. *J. Am. Chem. Soc.* **1972**, *94*, 3554.

CR940029J